Chapter 7

The importance of nanostructured materials for energy storage/conversion

M.J. Mochane*[1], T.C. Mokhena[1], L.Z. Linganiso[1], T.E. Motaung[1], T.H. Mokhothu[2], and A. Mtibe[2]

[1]*Department of Chemistry, University of Zululand (KwaDlangezwa Campus), Private Bag X1001, 3886, South Africa*

[2]*Council for Scientific and Industrial Research (CSIR), Nonwovens and Composites Research Group, 4 Gomery Avenue, Summerstrand, South Africa*

Abstract

The finite nature of fossil fuels and concerns over greenhouse effect make the effective utilization of energy and conservation key issues. Using environmentally friendlier materials to either produce or store energy become extremely important to overcome the disparity between the energy supply and demand. Nowadays, the replacement of conventional energy with renewable sources such as hydrogen storage, thermal storage, lithium batteries and supercapacitors received relentless interest. Nanomaterials garnered much interest because of their superior properties such as large surface area, favourable carrier properties, mechanical stability, and both high electrical and thermal conductivity resulting from their nanosized structures. Due to their structural diversity and excellent properties, nanostructured materials and their composites have been extensively studied for energy storage/conversion related applications including photo-catalyst for water splitting, hydrogen storage materials, and thermal energy storage materials, as well as electrode materials for various lithium batteries and supercapacitors. This chapter summarizes the recent developments, limitations and challenges of the nanostructured materials for energy storage/conversion applications. The limitations and challenges of using nanostructured materials to enhance the performance of the energy storage materials have also been addressed.

Keywords: fossil fuels, energy storage, lithium-ion battery, greenhouse gases

Corresponding authors: mochane.jonas@gmail.com; mokhenateboho@gmail.com

7.1 Introduction

The global utilization of fossil fuels grows at a disturbing and unsustainable rate. The release of greenhouse gases and other toxic pollutants are at an unacceptable elevation which is not good for environmental concerns. In most regions of the world, direct solar radiation is thought as a prospective source of energy storage. The future stability of our society depends on the alternative energy sources that are renewable and environmental friendly [1,2]. Researchers globally are investigating on finding a new and renewable energy sources. Energy storage is important in a sense that it reduces the gap between energy supply and demand; it further enhances the reliability and performances of energy systems [3]. This could lead to saving of fuels and making cost effective systems by storing the wastage of energy. To make sense of the whole discussion, it is clear that storage will probably enhances the performance of a power plant for an example, thereby loading level and higher efficiency which would result in energy conservation and reduced generation cost overall [4].

Throughout our existence as human beings, our advances have been based on the discovery, development and employment of new materials. Materials have been considered as the main the core of all technologies as most technological discoveries have been achieved through the development of new materials [5]. The recent technologies are such that the nanomaterials are heavily starting to play a significant in the production of new fields of science and nanotechnologies. In order for us to develop technological discoveries in the production of effective renewable energy storage/conversion, we need nanomaterial to fully develop the potential of renewable energy. As such, the potential of nanomaterials must be discovered at a more fundamental level.

Nanotechnology applications and development in the field of energy storage include (i) nanostructured materials and separators for super capacitors and batteries. This includes lithium ion batteries for automotive drives and stationery mass materials and electrolytic systems, designation of new types of batteries such as lithium air and lithium sulphur. Carbon nanotubes based electrode materials for super capacitors and batteries (ii) nanoporous adsorption storage for mobile gas storage (hydrogen, natural gas). A battery is known as container consisting of one or more cells, in which chemical energy is converted into electricity and used as a source of power. In this chapter different types of energy storage

which include lithium-ion battery, sodium air battery, supercapacitor and metal hydrid storage are discussed.

7.2 Classification and production of nanomaterials

Nanotechnology is a core of multidisciplinary science that has roots in almost all the fields of Science and Technology. It discusses the production of structures at a very small scale and on the level of nanometers. Nanoscience is the research of fundamental principles of structures having sizes between 1 and 100 nm. Generally, nanomaterials are the main core of nanoscience together with nanotechnology. The study of nanomaterials is a broad and exciting area of research and development that has been growing significantly worldwide in the past few years. Nanomaterials are not really new materials, even though they may appear as new materials. Volcano dust has been existing for some time in nature. The release of ash during volcano emission can reach temperatures over 1,400°C and has a very complex structure consisting of solid and liquid particulate matter lifted by the hot gas current [6]. The distribution of ash into the atmosphere resulted in a gas temperature lowering and gas composition changes which led to the accumulation of the particles as either clusters thorough chemical reactions or based on electrostatic forces of attraction.

There are also other man made nanoparticles such as carbon based materials and fumed Titania (TiO_2). One of the most common ways of classifying nanomaterials is to differentiate them according to the production method. There are two kinds of methods used for the production of nanomaterials which includes physical and chemical methods. The physical-mechanical method produces nanoparticles in the nanometer sized range by milling or grinding larger particles (**Figure 7.1).** A common name for this method is the top-down way of making nanomaterials. The mechanical-physical crushing methods for producing nanoparticles involve various milling, whereby milling uses thermal stress and is energy intensive.

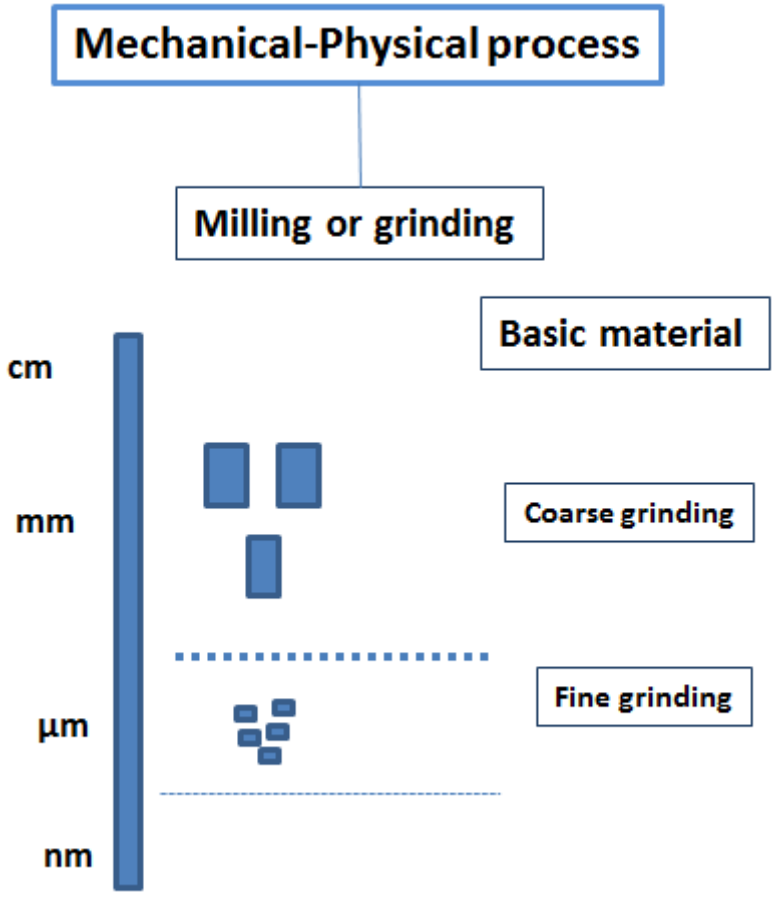

Figure 7.1 Overview of mechanical-physical nanoparticle production processes

The physical method is subdivided into mechanical and phase-change methods as depicted in **Figure 7.2**. It is noted that both kinds of physical methods doesn't results in the chemical change for the production of nanoparticles. The physical-phase change method involves the production nanoparticles *via* phase change process. Typical examples of physical-phase method include direct precipitation, whereby a material in solution is precipitated into a powder of nanoparticles, and as well as laser ablation in which the vaporized material is condensed into a solid nanomaterial.

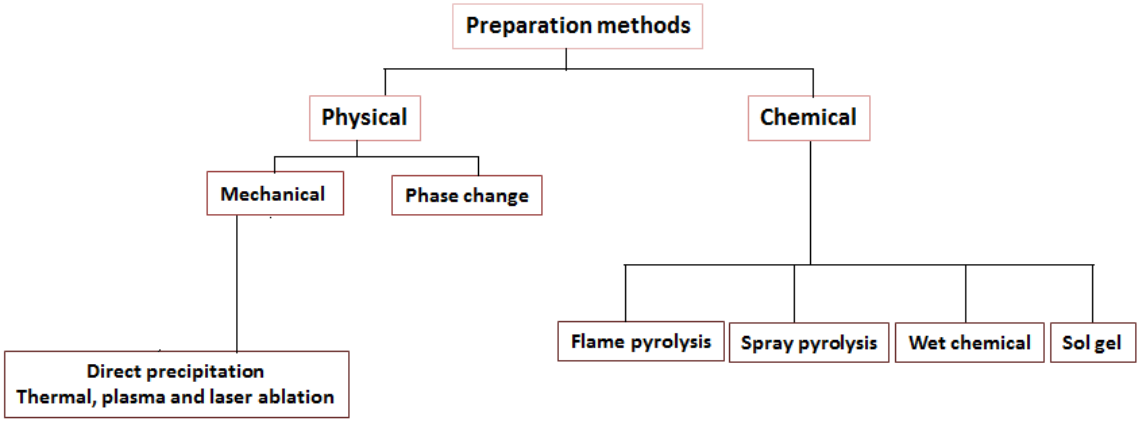

Figure 7.2 Schematic presentation of the methods used for the production of nanomaterials

Figure 7.3 shows an experimental set-up for colloid preparation by laser ablation in solution. The basic concept of laser ablation occurs as follows: When the laser beam is concentrated on the surface of a target material in liquid phase, the temperature of the irradiated spot quickly increases, vaporizing the target material. Due to the increasing in temperature, the collision of the vaporized species and the neighbouring molecules result in the excitation of the electron state together with light emission and production of electrons as well ions, forming laser-induced plasma spreading out in a shape resembling a feather [7]. The plasma structure depends on a couple of factors such as the target material, ambient media, pressure and laser condition. One could mention that the low-pressure laser ablation gas is preferred for generation of a large plume and as a result small particles are produced. The ambient media happen to be important in laser ablation experiments because laser generated particles as mentioned elsewhere in this document react with the surrounding molecules to form complexes such as oxides and other unwanted materials.

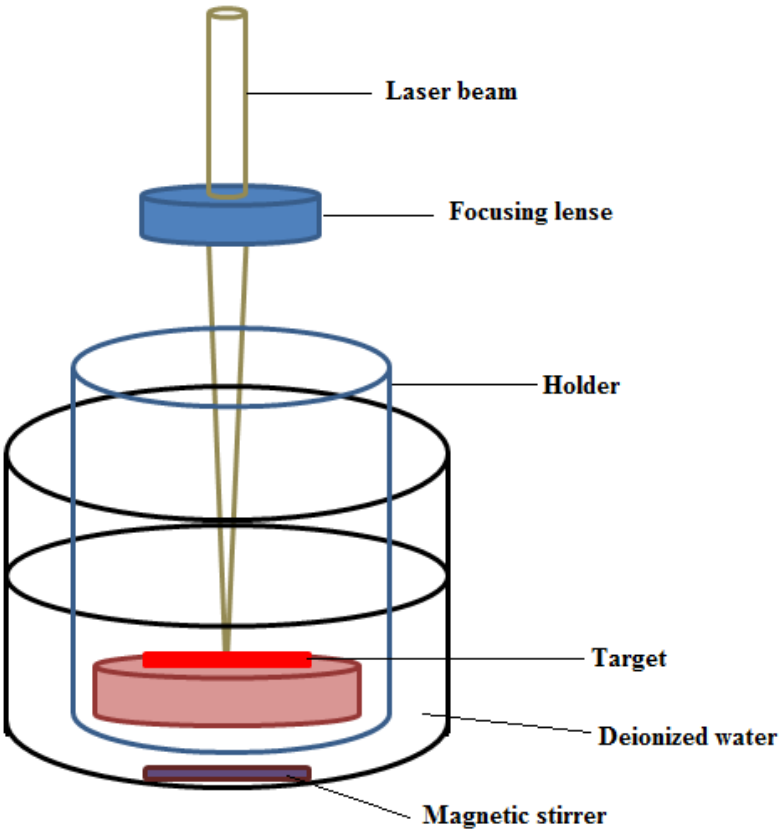

Figure 7.3 Experimental set-up for colloid preparation by laser ablation in solution

Generally, the chemical methods require that the nanomaterial should be synthesized from initial material which is chemically different from the target material. The chemical method is typical bottom-up approach and different types of chemical methods are shown in **Figure 7.2.** The bottom-up method is built on physico-chemical principles of molecular or atomic self-organization. The advantage of this method is that it produces selected complex structures from atoms or molecules with better controlling sizes of shapes and size range.

7.3 Different types of energy storage nanomaterials

7.3.1 Lithium-ion battery

Rechargeable battery technology has come a long way since its introduction in the early 1990s. According to the literature [8], there is a moderate increase in the energy density of lithium ion systems **(Figure 7.4)** in the last two decades since their introduction. There are a lot of rechargeable batteries which includes nickel–metal hydride, lead acid, lithium ion

which has been used for electric vehicle application. Amongst the above mentioned energy storage batteries, lithium ion battery has been the most attractive choice for automobile industries despite the fact that it is expensive [9]. Lithium ion batteries have been widely used since the early 1990s. Lithium-ion battery has shown productive performance in the application of automobile, cellular phone, note book computers because of better power and energy density compared with other energy storage devices. Furthermore, the lithium-ion battery has been significantly used because of attractive characteristics such as high efficiency, long cycle life, low discharge rate and high voltage. Another emerging application for Lithium-ion technology is in battery electrical energy storage systems for smart grids that are powered by traditional energy sources like coal, as well as intermittent renewable energy sources like solar and wind.

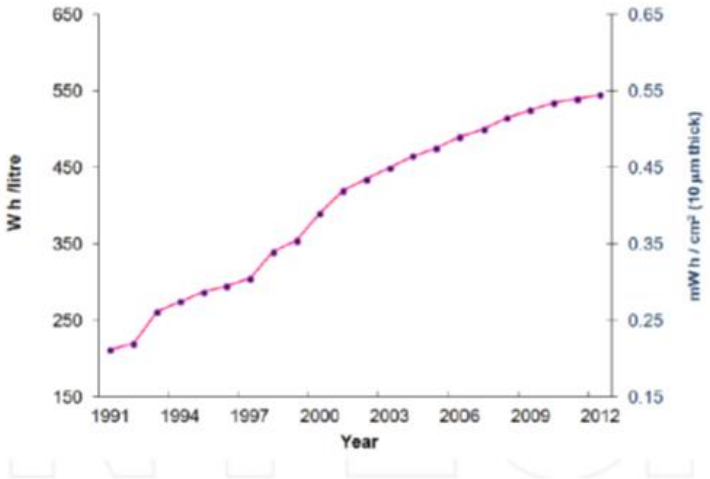

Figure 7.4 Lithium ion energy density improvements since 1991. ©2014 Rohan JF, Hasan M, Patil S, Casey DP, Clancy T. Published in [8] under CC by 3.0 license. Available from: http://dx.doi.org/10.5772/57139.

Ordinary Lithium-ion battery starts as a 10-50 micron sized particles which are coated onto aluminium or copper current collectors together with conductivity enhancers and binders. **Table 7.1** illustrates the main constituents of lithium-ion battery and their characteristics. The most employed cathode electrodes include lithium cobalt oxide, lithium nickel oxide, Lithium nickel cobalt aluminium oxide, Lithium manganese spinel, and Lithium iron phosphate. Carbon-based materials have been the most favoured choice for anodes, with some version of graphite being utilized in a majority of the commercially available lithium-ion batteries. Natural graphite is the obvious choice as anode material compared to other carbonaceous

materials because it is inexpensive. Moreover, the graphite anode electrode display a high capacity through its high degree of crystallinity as well as less profile compared with lithium [10,11]. Graphite as a dominating anode material consist of two phases i.e. predominantly hexagonal (2H), with a small fraction of a rhombohedral (3R) phase which are responsible for the intercalation of lithium ions [10,11].

Figure 7.5 shows a schematic presentation of typical lithium-ion battery. The cell consists of five regions, including composite negative electrode (anode), composite positive electrode (cathode), separator, and two electrode current collectors; made of copper and aluminium respectively. The two electrodes (anode and cathode) are divided by an electrolyte separator such as lithium hexafluorophosphate. The following half-reaction takes place at cathode and anode respectively:

$$LiMO_2 \leftrightarrow Li_{-z}\,MO_2 + zLi^+ + ze^- \qquad \textbf{(7.1)}$$

$$zLi^+ + ze^- + 6C \leftrightarrow Li_zC_6 \qquad \textbf{(7.2)}$$

Equations 7.1 and **7.2** are in units of moles, *z* is the coefficient for a complete reaction, whereas M depicts the metal in which lithium oxide is formed.

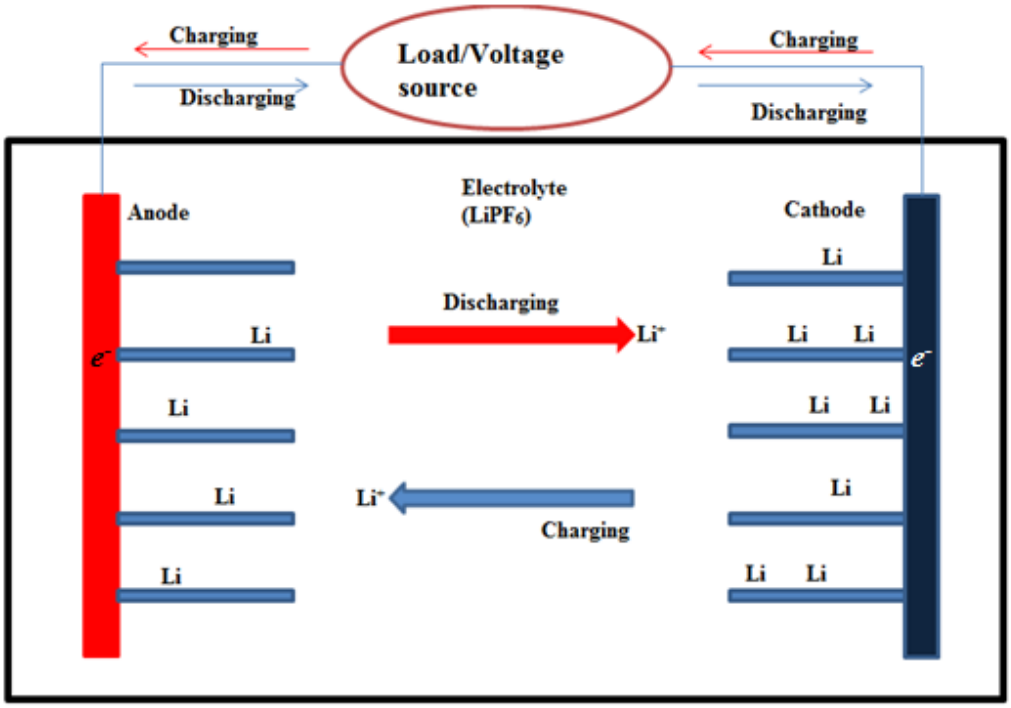

Figure 7.5 A schematic presentation of a typical lithium-ion battery.

During the process of charging, the voltage exerted across the electrodes proceeds the half reaction in the forward reaction i.e. from cathode to anode as it is depicted in **Figure 7.5**. The metal in the lithium metal oxide which is represented in the cathode is reduced to form lithium ions which are liberated in the electrolyte. The liberated ions diffuse through the electrolyte and are received into the carbon/graphite anode. During the formation of ions, electrons are produced to provide necessity for charge neutrality. According to the literature the electrolytes does not necessarily facilitate the conduction of free electrons through the system [12]. The electrons are moved across a wire connecting the two electrodes to provide necessary electrons required for the insertion of Li ions into the anode. During discharge, there is deintercalation between the negative electrode particles and solution. The electrons travel from anode to cathode during discharge process which causes positive current to originate from the cathode, as result the cathode act as positive terminal of the cell. Energy is stored in the electrodes in the form of Li-intercalation compounds.

Table 7.1 Major component of lithium-ion batteries and their characteristics [9]

Abbrev	LCO	NLO	NCA	NMC	LMO	LFP	LTO
Name	Lithium Cobalt oxide	Lithium nickel oxide	Lithium nickel cobalt aluminium oxide	Lithium nickel, manganese cobalt oxide	Lithium manganese spinel	Lithium iron phosphate	Lithium titanate LMO, NCA
Positive electrode	$LiCoO_2$	$LiNiO_2$	$Li(Ni_085Co_{0,}1Al_005)O_2$	$Li(Ni_033Mn_{0,}33Co_0)O_2$	$LiMn_2O_4$	$LiFePO_4$	LMO,NCA
Negative electrode	Graphite	Graphite	Graphite	Graphite	Graphite	Graphite	$Li4Ti_5O_{12}$
Cell voltage (V)	3.7-3.9	3.6	3.65	3.8-4.0	4	3.3	2.3-2.5
Energy Density (Wh/kg)	150 mA h/g	150	130	170	120	130	85

7.3.1.1 The advantages of nanomaterials in lithium-ion battery applications

The designation of a nanomaterial electrode as a Lithium-ion storage material would provide significant improvement in energy, power, and cycle life. The advantage of using nanoparticles as an electrode for lithium-ion battery applications for active energy storage can be seen in two (i) reduced diffusion distance for the lithium-ion particle core to the surface where it transfers to the electrolyte and (ii) nanoparticles provides high surface area because of their size as a result there will be higher electrode-electrolyte contact area [13]. The reductions in the particle size into the nanoscale significantly reduce the mechanical stresses caused by volumetric expansion and contraction during charge and discharge. The majority of lithium-ion cathode materials such as $LiCoO_2$, $Li(Ni_033Mn_{0,}33Co_0)O_2$ and $LiMn_2O_4$ consists of lithium and metals more especially the transition ones. The complex compound i.e. lithium and other transition metals may be required to be heated in some cases to achieve the desired oxide or phosphate composition. Heat treatment of large particles in comparison to smaller particles may be heavy and requires large-scale of energy, with a possibility of a different thermal characteristics in comparison to the bulk. If the particle size is large, there will be improper heat treatment which will result into nonhomogeneous composition in the material and hence decline in performance. The use of nanomaterials makes it is easier to sustain a homogenous thermal behavior throughout the material and thereby producing homogenous composition without applying a lot of energy to the complex material.

7.3.1.2 Carbon based nanomaterials for lithium-ion batteries

7.3.1.2.1 Carbon based materials

Carbon is the sixth element in the periodic table of elements, and it became very important in scientific research because it can combine with itself and other chemical elements in different ways [14]**.** Carbon exists in three forms, known as amorphous carbon, graphite and diamond. In nature, carbon is available in more quantity as coal. There are also man-made carbon materials based on the required application which include: synthetic graphite, synthetic diamonds, adsorbent carbon, cokes, carbon black, and diamond-like carbon [14]. Diamond, graphene, graphite and fullerenes related materials (which include carbon nanotubes and carbon nanofibers) are well allotropes of carbon. Carbon based materials are preferred

choices in many applications including energy storage in lithium-ion batteries for energy storage in comparison to metallic materials because of high thermal conductivity values, less corrosion and cyclic reversibility [15]. Moreover, carbon based materials have the ability to provide active reaction sites and high specific area which allows the addition of stable active materials for high or better electrochemical performances [15].

7.3.1.2.2 Graphene nanoparticles

For the past three decades since the breakthrough of anode materials for lithium secondary battery resulting in the birth and commercialization of lithium ion battery, research on anode materials has been the main focus. There are a lot of anode materials that has been investigated so far including graphitic carbon, amorphous carbon, nitrides, tin oxides and tin-based alloys [16]. However, to our knowledge carbon based materials are still the dominating one available in the market. The reason for the use of carbon materials in this electrode is because (i) they exhibit both higher specific charges and more negative redox potential than most metal oxides (ii) Show better cycling performance than Li alloys because of their good dimensional stability. The insertion of lithium ions into the carbon based materials is known as the intercalation process according to **Equation 7.3** below:

$$Li_a\ C_n \leftrightarrow aLi + ae + C_n \qquad \textbf{(7.3)}$$

The carbon host material has a good electrochemical reduction; as a result the lithium ions can easily penetrate into the carbon and form a lithium/carbon intercalation compound Li_aC_n and the reaction in equation is reversible. Carbon based materials that are capable of reversible lithium intercalation can be classified into two groups i.e. graphitic and non-graphitic. Graphitic carbons are defined as carbon materials consisting of the element carbon in the allotropic form of graphite. From crystallographic definition, graphite is known as carbons having a layered lattice structure with perfect stacking order of graphene layers. The non-graphitic carbonaceous materials consist of carbon atoms that are mostly arranged in a planar hexagonal network without being close to forming crystallographic order in the c-direction. Graphite has been the main commercially used anode for lithium ion batteries as shown in **Table 7.1**. According to the literature, graphite experiences a limited theoretical capacity of 372 mA h g^{-1} which is less than what is required of high energy capacity [17]. A

lot of attempt was done in developing other carbonaceous materials in order to obtain better performance. Graphene showed some distinctive advantages compared to graphite in energy storage applications. Graphene is a single-atom thick, two-dimensional sheet of sp^2 bonded carbon **(Figure 7.6)**. The specific surface area of graphene is 2620 m^2g^{-1} which is much higher than that of graphite with values approximately 1300 and 10-20 m^2g^{-1}. The large surface area of the graphene nanoparticles in comparison to the graphite particles provides more electrochemical reaction active sites for energy storage. In comparison to graphite, graphene nanosheets are also flexible which is beneficial for constructing flexible energy storage [18].

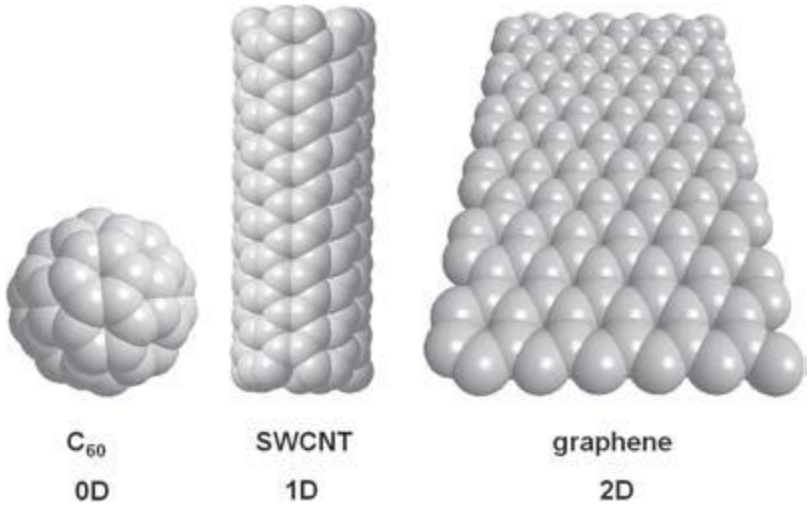

Figure 7.6 The three forms of carbon: 0-dimensional, fullerene C_{60}; 1-dimensional, single-walled carbon nanotube; and 2-dimensional, graphene sheet. Reprinted with permission from [18]. Copyright (2009) John Wiley and Sons

A lot of studies investigated the electrochemical properties of graphene as an anode for lithium ion batteries (LIB) and the results are summarized in **Table 7.2**. Guo *et al*. [19] reported that the graphite nanoparticles (GNS) exhibited a high reversible capacity of 672 mAh g^{-1} and a good cyclic performance. The authors attributed this observation to the storage of lithium on both sides of the graphene surface. Furthermore, another study [20] showed the storage of lithium ion on both surfaces of the GNS as well as the edges and covalent sites [20]. One of the advantages of graphene nanoparticles is the large surface areas which can provide more electrochemical reaction active sites for energy storage. The lithium storage

properties of graphene nanosheets (GNS) materials as high capacity anode material for rechargeable lithium battery were investigated by Yoo and co-workers [21]. The authors reported a specific capacity of GNS to be approximately 540 mAh g^{-1} which is much higher than that of graphite as it is revealed in **Figure 7.7**. The authors from the same study observed higher capacity values (730 and 784 mAh g^{-1}) by embedding CNTs or fullerene macromolecules into the graphene layers to increase the interlayer distance which probably provided additional sites for the accommodation of lithium ions. The electrochemical properties of graphene paper as anode electrode in lithium batteries was investigated in study [22]. Generally, the graphene papers were found to be mechanically strong and electrically conductive with a very high young modulus value (41.8 GPa). However, the electrochemical properties were found to be poor in comparison to the mechanical properties of the graphene paper. The discharge capacity was initially reported to be 298 mA g^{-1} which was less than the theoretical capacity of graphite, decreasing to 240 mAh g^{-1} after 50 cycles. The results conclude that the graphene paper is not suitable for application as the anode material in a rechargeable lithium ion battery.

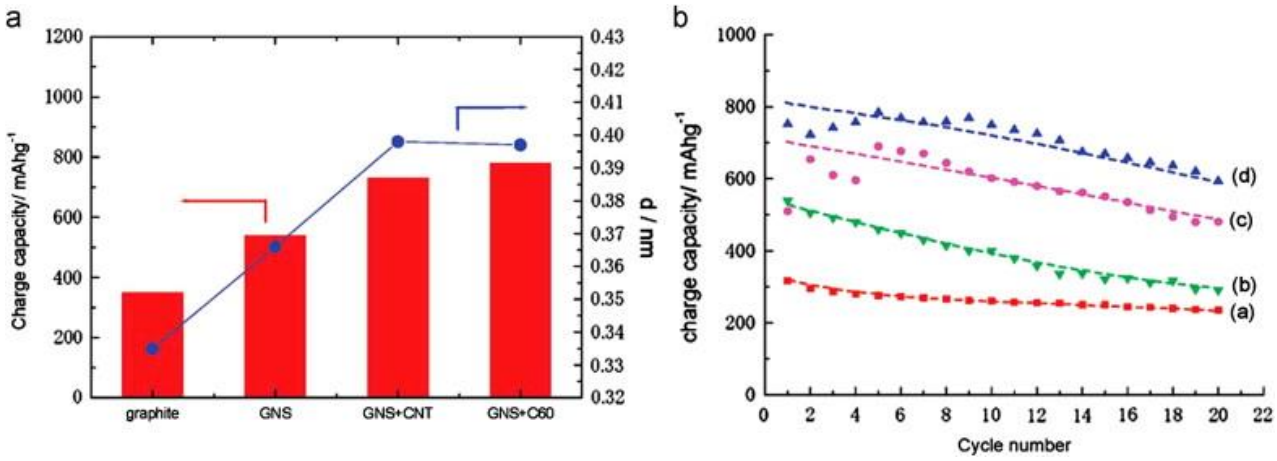

Figure 7.7 **(a) Relationship between the d-spacing and charge capacity of GNS families and graphite. (b) Charge/discharge cyclic performance of (a) graphite, (b) GNS+CNT, and (d) GNS + C_{60}. Reprinted with permission from [21]. Copyright (2008) American Chemical Society.**

The method of preparation of graphite nanosheets has significant impact on the electrochemical properties of the resultant LIBs. Lian *et al.* [23] investigated large reversible capacity of high quality graphene sheets (4 layers) as an anode material for lithium-ion batteries. The authors reported the first specific capacity of the graphene sheets as high as

1264 mAh g^{-1} **(Figure 7.8)** at a current density of 100 mAh g^{-1}. The reversible capacity of graphene sheets with fewer layers is much higher than the previously reported literature [21] with graphene nanosheets (540 mAh g^{-1} at low current density of 50 mA g^{-1}). Comparison of the two studies revealed that the prepared graphene sheets with fewer layers (4 layers) have an intensive potential as a candidate of anode materials with high reversible capacity, good cycle performance and high rate discharge/charge capability. A possible reason for higher electrochemical properties for fewer graphite nanosheets was attributed to a large surface area and curled morphology of graphene sheets with fewer layers provided more lithium insertion active sites, such as edge-type sites and nanopores. Similarly, Wang and co-workers [24] reported that less graphite nanoparticle layers (5 layers) produced at low temperature (300°C) showed remarkable electrochemical performance in comparison to 13 layers obtained at 800°C. This was attributed to a higher specific surface area of lesser GNS layers than more graphene layers. In another study [25], graphene nanosheets were prepared from graphite oxide by two different methods i.e. Thermal exfoliation at different temperatures and wet chemistry using aqueous N_2H_4 and KBH_4 as the reducing agent. Generally, the two systems produced a high irreversible specific capacity irrespective of the method used for preparation of GNS. However, when comparing the two reducing agents, the GNS synthesized with N_2H_4 showed better performance in comparison to KBH_4. The authors also reported that the GNS produced with KBH_4 and the thermal temperature of 800°C resulted in poor electrochemical performance of the GNS.

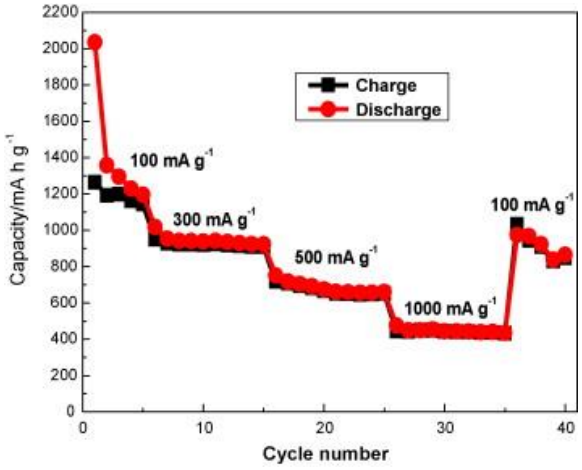

Figure 7.8 **Cycle performance of graphene sheets at the current densities from 100 mA g^{-1} to 1000 mA g^{-1}. Reprinted with permission from [23]. Copyright (2010) Elsevier**

Graphene nanoparticles just like any other nanoparticles suffer from agglomeration and re-stalking due to the van der Waals as a result decreasing the electrochemical performance of graphene nanoparticles in LIBs [26]. The following section discusses recent progress in the surface modification of graphene anodes by metals and/or metal oxide.

7.3.1.2.3 Surface modification of Graphene nanoparticles anodes

Recent studies have investigated various methods of surface modification of graphene electrodes such deposition of metals, metal oxides, coating with polymers [27-30]**.** Depending on the modification method, the following improvement may be attained: (i) smoothing the active edge surfaces by removing defects on the graphene surface (ii) forming a dense oxide layer on the graphene surface (iii) increasing the electronic conductivity (iv) Inhibiting structural changes during cycling. According to a reported literature above, deposition of certain metals or metal oxides which are host sites for lithium storage and improvement of the capacity of the anode. Several electrochemical properties (anode electrode) of the graphene with other nanoparticles or metal oxides are shown in Table 2 designed from different literatures. A lot of literatures reported [27,31-34] on the graphene/metal oxides for lithium ion batteries. **Figure 7.9** shows a typical preparation of the graphene/metal oxides composites.

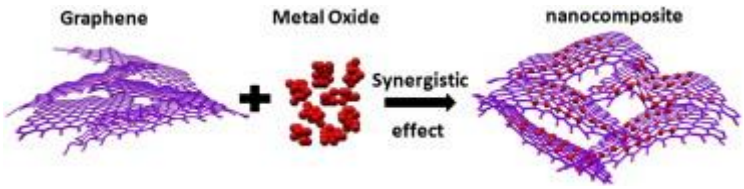

Figure 7.9 Schematic of the preparation of graphene/metal oxide composites with synergistic effects between graphene and metal oxides [26]. Copyright (2011) Elsevier

The aim of using both graphene and metal oxides for anode electrode is to lower the electrode problems of the individual components being the main active site, however utilizing the advantages of both graphene and metal oxide as active sites to improve the overall electrochemical properties of the system. In the composite both graphene and metal oxides provides different functions i.e. Graphene offer chemical functionality and compatibility whereas metal oxides provide high capacity. The resultant composite similar to a combination of blends provide a new material which is a combination of graphene and metal

oxide with new properties and functionalities. Generally, from the expectation point of view, metal oxide is expected not decrease agglomeration of graphene nanosheet only but also to increase the surface area of graphene nanoparticles leading to better electrochemical properties. Cobalt monoxide (CoO) quantum dot/graphene nanosheet composite was prepared with facile ultrasonic synthesis for LIBs [32]. The resultant CoO/graphene composite showed high performance as anode material for lithium ion battery with a reversible specific capacity of 1592 mAh g^{-1} after 50 cycles. The improvement in electrochemical properties of the system was ascribed to a well dispersed nanosized CoO quantum dots on conductive graphene matrix **(Figure 7.10)** which enhanced the active sites for lithium insertion, shorten the diffusion length for lithium ions which is favourable for high capacity and rate capacity.

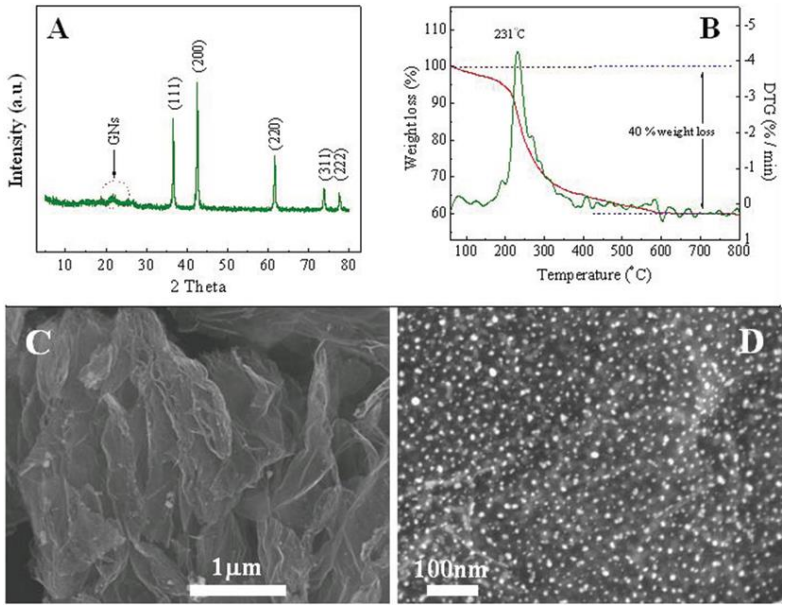

Figure 7.10 (A) XRD pattern, (B) TGA, and (C,D) SEM images of the CQD/GN composites Reprinted with permission from [32]. Copyright (2012) American Chemical Society.

Most recently, stannic oxide (SnO_2)/graphene nanocomposite paper (as both anode for lithium ion battery) were synthesized by the so called facile hydrothermal method [27]. The prepared nanocomposite in this case was chosen with the aim of forming flexible lithium-ion batteries. The flexible SnO_2/graphene paper showed a discharge capacity of 1195 $mAhg^{-1}$ after 10 cycles and maintained at 1094 $mAhg^{-1}$ after 80 cycles. Based on the result above it was concluded that the SnO_2/graphene paper is one of the candidate for flexible lithium-ion batteries. Similarly, graphite nanoparticles coated with α-Fe_2O_3 [29] improved the electronic conductivity and diminishing the volume expansion, also proving enough active sites for lithium storage and shorten the lithium ion diffusion pathway. This has suggested that the α-

Fe_2O_3 coated graphite nanoparticles composite can be used as a potential anode material for high cyclic stability and long life lithium ion battery. The electrochemical properties of recent studies of graphene/metal oxide composite are shown in **Table 7.2.** Lately, a lot of studies investigated the performance of lithium ion battery in hybrid systems. Different systems (hybrids) were employed such as nanowire-graphene, Bi_2Te_3-nanoplate/graphene nanosheets [35], and phosphorus-graphene nanosheet hybrids [36] as anodes for lithium-ion batteries. By hybrid materials we are of the understanding that the composites consist of two constituents that are at nanometer or molecular level. A successful phosphorus-graphene nanosheet hybrid was prepared by ball milling method which is regarded as the low-cost method [36]. In this study, the phosphorus particles were grounded into smaller particles and hybridized with graphene nanosheets to form a 3D integrated structure. The authors reported a high specific capacity of 2362 mAh g^{-1} and outstanding capacity retention after approximately 300 cycles at room temperature. The specific capacity of 1623 $mAhg^{-1}$ was obtained at elevated temperatures (60 °C) after 200 cycles. Graphene nanosheet were also mixed with different complexes and doped with different materials for improving the electrochemical properties of LIBs and the results also are summarized in **Table 7.2**. Guo and co-workers [37] investigated the layer-by layer assembled composite of graphene nanosheets (GNSs) wrapped in monodisperse cobalt sulfide (CoS_2) nanocages for anode performances of lithium ion batteries. The monodisperse nanocages provided additional space to allow the volume changes, shorten lithium diffusion path and reduce agglomerations. As a result, the authors reported a high specific capacity 800 $mAhg^{-1}$ after 150 cycles at 100 mAg^{-1} and 697 $mAhg^{-1}$ after 300 cycles at 500 mAg^{-1}. Tang and co-workers [29] investigated the silicon nanoparticles enwrapped with N-doped carbon and combine with N-doped graphene and carbon nanotubes as an anode material for lithium ion battery. The composite delivered magnificent cyclic retention of 892.3 mAh g^{-1} after 100 cycles. The improved electrochemical performance was attributed to the well protected silicon nanoparticles and excellent conductivity provided by N-doping graphene and carbon nanotubes which may release the stress of the silicon due to volume expansion and decrease the transfer resistance of lithium ion in the anode electrode. However, most recently, FeP@reduced graphene oxide (FeP@rGO) prepared at mass ratio of of 1:5 (graphene oxide to $FeCl_3.6H_2O$) delivered a reversible discharge of 1000 mAh g^{-1} after. It should be noted that in this case graphene oxide which is a layer of graphene with oxygen atoms was the one attached to the $FeCl_3.6H_2O$. Improved electrochemical properties might open options for FeP@reduced graphene oxide as a potential application for advanced LIBs.

Table 7.2 Electrochemical properties of graphene and its synergy with other nanoparticles for lithium ion battery from recent studies

Graphene or graphene + other nanoparticles (anode)	**Performance improvements**	**Refs.**
Cu-supported graphene nanoflakes	Specific capacity of 165 mAh g^{-1} over 80 charge-discharge cycle	[30]
graphene nanosheets (GNS)	Capacity of 540 mAh g^{-1} which is higher than that of graphite	[21]
GNS + CNTs or fullerene	higher capacity values (730 and 784 mAh g^{-1}) by embedding CNTs or fullerene	[21]
SnO_2-graphene paper	Discharge capacity of 1195 mAh g^{-1} after 10 cycles	[27]
$NiCo_2O_4$/graphene	Higher reversible capacity and better cycling stability than $NiCo_2O_4$	[34]
MnO@graphene	Reversible capacity as high as 989.8 $mAhg^{-1}$	[33]
Fe_2O_3@graphite	Provided a specific capacity of 518,5 $mAhg^{-1}$ at current of 1000 mAg^{-1} (1000 cycles	[29]
Graphene + cobalt sulfide	Delivered a high capacity~800 $mAhg^{-1}$	[37]
Graphene paper	Discharge capacity dropping from 680 to 84 $mAhg^{-1}$	[22]
Graphene sheet	Specific capacity was as high as 1264 $mAhg^{-1}$ at current density of 100 mAg^{-1}	[23]
SiliconC@C/graphite	Charge/discharge showed a specific capacity of 919.0 $mAhg^{-1}$	[38]
Anatase TiO_2 Quantum-Dot/graphene	Great improvements in electrochemical properties	[31]
CoO Quantum Dot/graphene	Storage capacity of 1592 $mAhg^{-1}$ after 50 cycles	[32]
Carbon nanofiber/highly branched graphene	Hybrid material showed a reversible capacity of 300 $mAhg^{-1}$	[28]
Bi_2Te_3	Improved cyclic stability compared with Bi_2Te_3 alone	[35]

nanoplatelet/graphene		
$NiCO_2O_4$/graphene	$NiCO_2O_4$/graphene composites showed improved capacity and better	[34]
MoS_2-coated vertical graphene nanosheet	Compared with MoS_2-carbon black, MoS_2/VGNS developed on Ni foam showed enhanced electrochemical properties	[39]

7.3.2 Sodium Battery

Research has escalated in the exploitation of utilizing sodium as a replacement lithium ion for large-scale energy storage from the economic and ecological view-points. Sodium is cheaper when compared to lithium due to its almost unlimited availability [40,41]. Much effort has been dedicated in enhancing the performance of lithium batteries and to overcome some of its challenges such as the accumulation of the charge/discharge products which deteriorate the long-term performance of the battery [40,41]. Although much progress has been made on the latter, the possibility of using lithium for future energy generation seems to be overshadowed by its price and toxicity, making its applicability in large-scale energy storage impractical. Sodium ion batteries (SIBs), on the other hand, have a great potential to give a similar or even better performance than lithium-based batteries at a relatively low cost. Although sodium battery seems to be a suitable solution to replace lithium especially considering its low toxicity, the sodium-based batteries still experiencing similar challenges as for lithium. Some of these challenges include low efficiency and poor cycle life, and mostly overheating. Similar to lithium-based batteries, sodium batteries have the same energy storage mechanism in which charging involves the metal ions flows from the cathode (sodium-containing species) to the anode (carbon) through the electrolyte. The discharging process involves the reverse mechanism. Amongst all challenges faced by the sodium-based batteries (SIB), the formation of dendrite (which is predicted to more than lithium based batteries LIB), large volume change and sluggish diffusion kinetics have been the subject of research over the past years [40,41]. Different nanoscale materials with various shapes have been studied as the possible solution to overcome these challenges. In this case, the electrodes from various materials in the nanoscale were utilized in order to improve the performance of the battery [40,41].

It is of interest to note that the similarities of sodium and lithium could give the scientists an edge regarding many studies conducted on lithium; however due to their difference especially

their size (*viz.* 1.02 A for sodium and 0.76 A for lithium) could cause such discrepancy with regard to the materials used for lithium batteries. For example, the use graphite as anode material for sodium yields extremely low capacity, while remarkable results were reported in the case of lithium-based batteries when graphite is an electrode. In addition, sodium has high reactivity with low melting temperature and has the similar problems as lithium when it comes to formation of dendrite. A wide variety of nanomaterials have been tested to enhance the performance of the SIBs. It is of significant importance that the material used has to bear some valuable properties such as large energy for ion adsorption, high thermal stability, high electronic conductivity, high ion diffusion and good structural stability [42,43].

7.3.2.1 Carbon-based materials

Carbon-based materials received lot of interest as the electrodes for sodium battery with regard to their performance in lithium-based batteries. Despite that, their unique structural properties and abundant availability makes them very interesting materials to enhance the performance of the batteries for large-scale energy storage. For example, Liu *et al*. [44] developed a binder-free multilayer nanocomposites core-shell microfiber electrode consist of hydrothermal synthesized SnO_2 nanocrystal layer on conductive carbon cloth (SnO_2/CC) by surface coating. Further coating with ALD Al_2O_3 (Al_2O_3/SnO_2/CC) was carried out to prevent detachment of the active material. It was reported that SnO_2/CC exhibited charge capacity of 529 mAh g^{-1} and retained only 30% of initial capacity after 40 cycles, while Al_2O_3/SnO_2/CC exhibited charge capacity of 470 mAh g^{-1} and maintained a 371 mAh g^{-1} specific capacity at 100^{th} cycle.

Graphene is one of the interesting materials which can be utilized to grow different nanomaterials, especially for high performance electrocatalytic or electrochemical devices [40,45,46]. The unique features of graphene such as explained elsewhere in this document (*viz.* lightweight, high surface are and conductivity) add more value to the formulation in which the nanoparticles are grown). Yang *et al*. [46] synthesized graphene oxide using modified Hummers method. The reduction of graphene oxide (GO) was performed by ammonia and hydrazine. GO was mixed with SnSe in a weight ratio of 9:1 using ball milling. It was demonstrated that GO/SnSe composites exhibited enhanced reversible capacity of 590 mAh g^{-1} at a current density of 0.05 Ag^{-1} and rate performance of 260 mAh g^{-1} at a current density of 10 Ag^{-1}. The cycle stability with capacity retention of 98% over 120 cycles at a current density of 1 Ag^{-1} was achieved. Phosphorus features extraordinary capacity of 2596

mAh g^{-1} (i.e. 7 times higher than the commercial graphite); however its low conductivity and rapid structural degradation limit its application as electrode [47]. Recent study by Zhang *et al*. [47] reported that amorphous phosphorus/nitrogen-doped graphene exhibited remarkable stable cyclic performance and excellent rate capability. The electrode exhibited excellent capacity retention greater than 85% over 350 cycles, remarkable cycle stabity (0.002% decay per cycle from 2^{nd} to 350^{th} cycle with rate capability of 809 mAh g^{-1} at a current density of 1500 Ag^{-1}. Other possibility to improve the performance of graphene-based electrodes includes fabricating nanocomposites composed of graphene and transition metal dichalcogenides [48, 49]. This is as a result of improved electrical conductivity and structural stability of the composite electrode. A 2D $SnSe_2$/rGO nanocomposite prepared by hydrothermal method was reported by Zhang *et al*. [49]. A stable $SnSe_2$ layered structure was prepared from NaHSe solution for the first time. Nanocomposites ($SnSe_2$/rGO) exhibited initial discharge capacity of 756 mAh g^{-1} and a charge capacity of 660 mAh g^{-1}; and after 100 cycles a reversible capacity of 515 mAh g^{-1} was obtained. On other hand, Xiong *et al*. [48] used sulphur doped graphene and nanostructured Sb_2S_3 as an electrode for SIB. This composite exhibited a high specific capacity of 792.8 mAh g^{-1} at a current density of 0.05 A g^{-1}, good rate capability (591.6 mAh g^{-1} at 5 A g^{-1}) and excellent cycle life (83% capacity retention for 900 cycles at 2 A g^{-1}). It can be concluded that the inclusion of other nanostructured materials into the graphene layers can enhance the performance of the electrodes for sodium batteries. This in turn shows the potential as sodium batteries as another form for future large scale energy storage.

7.3.2.2 Non-carbon materials

Non-carbon materials include layered materials with excellent capacity which can potentially replace graphite [50-52]. These materials include transition metals with chalcogen such as S, Se and Te. Their chemical formula is usually expressed as MX_2 where *M* represents metal and *X* is chalcogen. The layers are bonded together by weak van der Waals forces which can accommodate ions and can further be exfoliated to accommodate more metal ions. Very few studies were conducted based on these materials as electrodes for sodium battery [50,51]. Mortazavi *et al*. [51] pointed out that Na ions were able to intercalate in MoS_2 which provided adsorption sites, however resulted in phase transformation from hexagonal phase to tetragonal phase giving rise to a maximum theoretical capacity of 146 and a low average electrode potential in the range of 0.75-1.25 V. Through barrier energy calculations of 0.68

and 0.28 eV for Na diffusion in 2H- and 1T-MoS_2 predicted moderately fast charge and fast discharge rates, respectively. It was concluded that 1T polytype deliver better electrochemical performance because of its inherited metallic electronic structure, higher capacity for Na ions and their faster mobilities. Lan *et al*. [50] studied molybdenum dinitride (MoN_2) as a potential candidate for Na-ion batteries anode. MoN_2 in T-type structure was studied using first principle method. It was found that sodium ions can adsorb onto the monolayer with maximum capacity of 864 mAh g^{-1} and diffusion barrier was 0.12 eV. Sodium ions were also found to adsorb separately without forming clusters which can contribute the overall performance of the battery especially during cycling. These materials (i.e. transition metal dichalcogenides) show potential for their application in stationary energy storage since graphite is not amenable for Na ions intercalation.

7.3.2.2.1 Borophene

Borophene is a metallic and lightweight material having two-dimensional (2D) structured sheets of boron [42,43,53]. It has a similar structure as grapheme hence the name borophene. It is capable of adsorbing sodium ions due to the availability of the adsorption site with strong binding energy. Mortazavi *et al*. [42] studied the capability of borophene as an anode material for Na storage. It was reported that the binding energy of 2.92 eV for Na was achieved which decreased with increase in Na content. Using Bader charge analysis to evaluate the charge transfer, it was pointed out that borophene with 2D structure have remarkable capacity of about 1380 mAh g^{-1} for Na which shows the capability of using borophene for rechargeable ion batteries. In addition, the thermal stability of the borophene up to 750 K also shows the capability of this material as anode material. Similarly, Liang *et al*. [53] studied the possibility of borophene as anode from two different structures, namely a closed-packed triangular B layer (B_{Δ}) and hexagonal voids or vacancies in B layer ($B_{\square}$). Using the first principle calculations to evaluate the potential of borophene as anode material for sodium ion, they found out that borophene has ad adsorption energy of -1.448 eV for all boron in the plane ($B_{\square}$) and -1.731 eV for B_{Δ}. The fully sodiated phase for respective $B_{\square}$ and B_{Δ} was Na0.083B and Na0.1B corresponding to a theoretical specific capacity of 248 mAh g^{-1} (496 mAh g^{-1} for two sides) for B_{Δ} and 298 mAh g^{-1} (596 mAh g^{-1} for two sides) for $B_{\square}$.

7.3.3 Sodium-air battery (SAB)

The operation process of air electrode relies on the reaction of oxygen either alkali metal to yield alkali oxides [41,54,55]. The cathode is usually made-up of porous carbon and/or porous metal to deliver current for oxygen reduction and also act as the host for the product. The discharge process involves the filling the voids with the oxide products and stops when all the voids are all filled. Oxygen reduction and oxidation processes rely on the catalyst coated onto the porous matrix. Thus it is of significant importance for the reaction between the oxygen and the alkali ions and electrons from conductive matrix for oxygen reduction at the catalyst sites during discharging. The reactions for sodium and oxygen can be expressed as follows: [54,56,57]

$$Na^+ + O_2 + e^- \rightarrow NaO_2 \qquad \text{E = 2.263 V} \quad \textbf{(7.4)}$$

$$2Na^+ + O_2 + 2e^- \rightarrow Na_2O_2 \qquad \text{E = 2.330 V} \quad \textbf{(7.5)}$$

$$4Na^+ + O_2 + 4e^- \rightarrow Na_2O \qquad \text{E = 1.946 V} \quad \textbf{(7.6)}$$

The products such as NaO_2, Na_2O_2 and Na_2O were found to accumulate on the cathode which affects the electrochemical cyclability performance of the battery. Therefore, it of significant important for the electrode to have proper porous structure with appropriate pore volume and pore size for adequate oxygen diffusion. Porous structured materials with large surface area were studied as suitable solution to overcome the accumulation of electrochemical products building up on the surface of the electrode as summarized in **Table 3**. Carbon-based materials have been mostly studied due to their unique properties such excellent electrical conductivity, high surface area and controllable structure and porosity.

7.3.3.1 Carbon-based materials

Although the research based on the sodium air battery is still in an infant stage the abundant availability of sodium makes it a potential candidate for large scale application. However, the discharge products (*viz*. sodium superoxide (NaO_2), $Na_2O_2H_2O$, Na_2O_2, NaOH and sodium carbonate (Na_2CO_3) have tendency of accumulating on the surface of the cathode electrode during charging/discharging cycle which affect the performance of the battery (**Table 7.3)** [58-60]. This has called upon new materials having porous structure to accommodate the discharged products without affecting the performance of the battery especially the blockage of the oxygen by the discharged products [61]. Morphological properties such as surface area, pore volume and size are of significant importance to improve the cycling performance by

reducing the over accumulation of the discharge products [58]. Various carbon based materials such as graphene, MWCNT, CNT [54,62] have been considered as promising cathodes for sodium air batteries. For example, Sun *et al*. [54] demonstrated that diamond-like carbon thin films can be used as electrode at room temperature. Specific discharge capacity of 1884 mAh g^{-1} (565 µAh cm^{-2}) at 1/10 C and 3600 mAh g^{-1} (108 mAh cm^{-2}) at 1/60 C was achieved using carbonate-based electrolyte.

Graphene nanosheets (GNS) received much interest due to their unique valuable properties such as large specific area, high electronic conductivity and high electro-catalytic activity towards the oxygen reduction reaction (OER). GNS were employed as an oxygen electrode for nonaqueous SAB by Liu *et al.* [63] and showed high discharge capacity of 9268 mAh g^{-1} at 200 mA g^{-1}. It was demonstrated that the electrochemical properties GNS for SABs was higher than that of the carbon electrode with high catalytic activity for both oxygen evolution reaction (OER) and oxygen reduction reaction (ORR). Graphene nanosheets synthesized by the oxidation of graphite powder were functionalized with platinum nanoparticles [61]. The platinum (Pt) nanoparticles (NPs) were grown by *in situ* on top of the nanosheets *via* hydrothermal method. It was found that the discharge capacity of platinum-based graphene reached 7574 mAh g^{-1} as compared to pure graphene with only 5413 mAh g^{-1} at the current density of 0.1 mA cm^{-2}. This was attributed to presence of the platinum nanoparticles (i) acting as oxygen reservoir because of the presence of large number of effective sites to adsorb oxygen, (ii) well-distributed Pt NPs accommodated discharged products, which alleviated the blockage of oxygen diffusion channels, and (iii) the high conductivity of the Pt NPs favours the conductivity of the electrode despite the insulating discharged products on its surface.

With its unique features such as large-surface area, high chemical stability, and excellent electrical conductivity, as well as good mechanical properties carbon nanotubes merit special interest as one of promising electrode for sodium air batteries. Jian *et al.* [64] prepared carbon nanotube paper as binder free air electrode. The paper displayed large discharge capacity of 7530 mAh g^{-1} at a current density of 500 mA g^{-1} with 0.5 $NaSO_3CF_3$/DEGDME as electrolyte. A rechargeable sodium-air battery operating at room temperature based on the carbon paper coated with multiwalled carbon nanotubes (MWCNTs) as oxygen electrode was studied recently by Elia, Hasa and Hassoun [65]. It was found that cell provided a discharge capacity of 4260 mAh g^{-1} leading to a theoretical energy density higher than 8000 Wh kg^{-1} due to the interconnected structure of MWCNTs suitable for discharge products deposition. The robust network aligned nitrogen-doped CNTs were able to accommodate the discharged products allowing their uniform coverage [66]. This promoted high cycling stability for at least 10 cycles at the current density ranging from 200 to 640 mA g^{-1}, and also sustained high

capacity at 600 and 640 mA g^{-1} for 44 and 55 cycles before dropping to 100 mA h^{-1}. A binder-free three-dimensional (3D) nanostructured electrode composed of vertically grown nitrogen-doped carbon nanotubes on carbon paper (NCNT-CP) was developed using a spray pyrolysis chemical vapour deposition by Yadegari *et al*. [62]. CP was covered by randomly oriented fibres with diameter of around 10 µm exhibiting a 3D structure with diverse pore sizes (**Figure 7.11a**). After nitrogen-doped CNT were grown on carbon paper (CP) a uniform layer of CNTs with the length around 10µm covered the carbon fibres (**Figure 7.11b-d**). TEM images revealed bamboo-like structure with stacked-cone structure (i.e. characteristic of NCNTs). NCNT-CP composed of micropores and mesopores (as confirmed by BET analyses **Figure 7.11g-h**) which are essential for oxygen diffusion and sodium ions transportation while accommodating discharged products. The NCNT-CP electrode exhibited a specific capacitance 17 times higher than bare CP (**Figure 7.12a**) due to its ability to accommodate discharge products while allowing continuous oxygen and sodium ions supply onto the surface of the electrode. It was established that the specific capacity reduces by 1.7 times when the discharge current density increases (**Figure 7.12b**) corroborating that the electrode had an appropriate structure for air breathing. In comparison with other electrodes based on CNTs from literature, the NCNT-CP performed better as shown in **Figure 7.12c**.

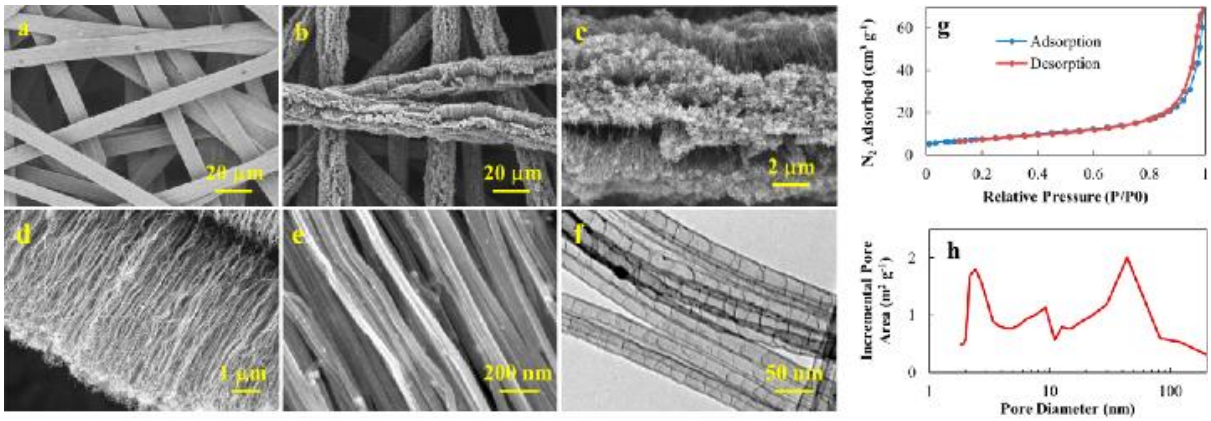

Figure 7.11 **(a-e) SEM and (f) TEM micrographs of (a) pristine CP and (b-f) NCNT-CP air electrode synthesized *via* SPCVD method for 3 min; (g) nitrogen adsorption/desorption isotherm of the synthesized NCNT-CP air electrode; (h) pore size distribution plot of the NCNT-CP air electrode. Reprinted with permission from [62] Copyright (2015) American Chemical Society.**

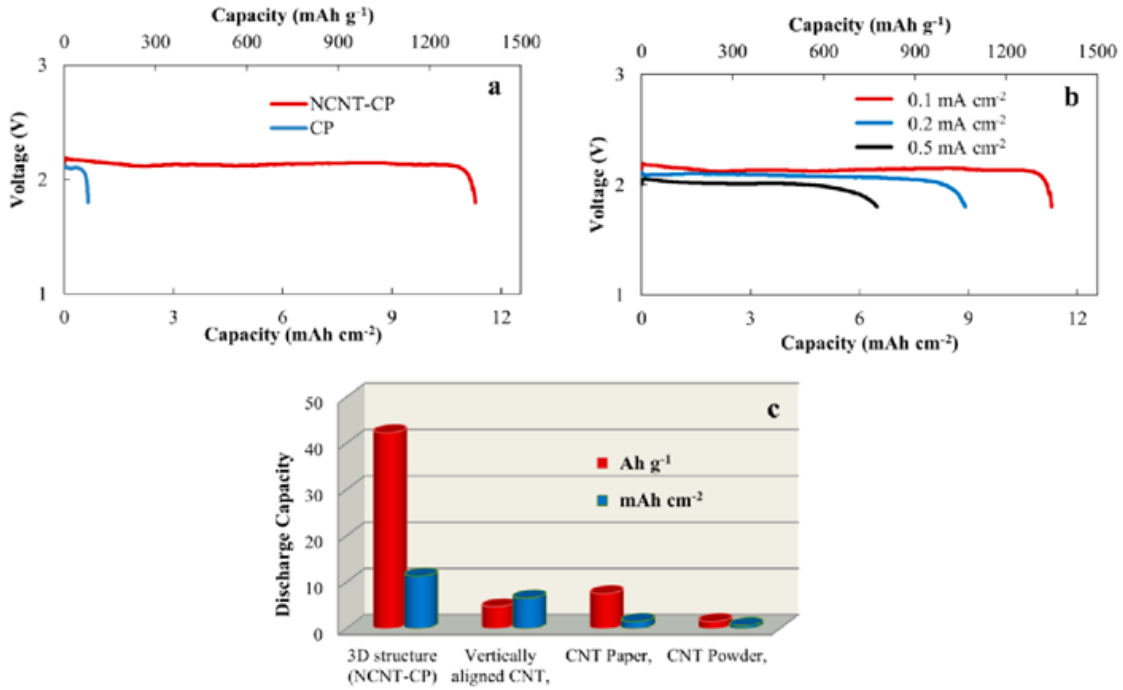

Figure 7.12 **(a) Discharge curves of pristine CP and NCNT-CP air electrodes (NCNT length of 10 µm) at a current density of 0.1 mA cm^{-2}. (b) Discharge curves of NCNT-CP air electrodes obtained at different current densities of 0.1, 0.2, and 0.5 mA cm^{-2}. (c) The specific capacities are calculated based on the geometric surface area (mAh cm^{-2}) and also based on the total weights of CP and NCNT-CP electrodes (mAh g^{-1}); the specific capacity for NCNT-CP and other CNTs containing air electrodes with different architectures including powder-based, CNTs paper, and vertically aligned CNTs from the literature. Reprinted with permission from [62] Copyright (2015) American Chemical Society.**

Table 7.3 Recent reports on the electrode for Na-air batteries

Electrode	Electrolyte	Air	Specific capacity	Discharge product	Ref.
Ordered Mesopous carbon (OMC)	0.5M $NaSO_3CF_3$/PC	oxygen	500 $mAhg^{-1}$ (100 mAg^{-1})	Na_2CO_3	[58]
Graphene nanosheets (GNS)	0.25M $NaPF_6$/DME	Dried air	9268 $mAhg^{-1}$ (200 mAg^{-1})	Na_2O_2	[63]
MWCNT	0.5M $NaSO_3CF_3$/TEG-DME	Oxygen	4260 $mAhg^{-1}$(100 mAg^{-1})	NaO_2	[65]
GNS-Pt			7574 $mAhg^{-1}$ (0.1 mA cm^{-2})	Na_2CO_3	[61]
CNT paper	0.5M $NaSO_3CF_3$/DEGDME			$Na_2O{\cdot}2H_2O$	[64]
Nitrogen-doped CNTs (NCNT)	0.5M $NaSO_3CF_3$/DEGDME	Dried air	1887 $mAhg^{-1}$ (25 mAg^{-1})	Na_2O_2 and NaO_2	[66]
Nitrogen-doped carbon nanotubes/ carbon paper (NCNT-CP)	0.5M $NaSO_3CF_3$/DEGDME	Oxygen	-	Na_2O_2 and NaO_2	[62]

7.3.4 Supercapacitors

Supercapacitors have low energy density as compared to other energy storage devices (*viz.* batteries and fuel cells), however they can be used as part of these energy storage materials. It is recognized that the improvements regarding their energy density can revolutionize the future of energy storage devices [67, 68]. In supercapacitors energy is stored in two different mechanisms, i.e. capacitive and pseudocapacitive. The capacitive process (non-Faradaic) relies on the charge separation at the electrode and electrode interface, while pseudocapacitive process (Faradaic) depend on redox reactions that occur on the electrode materials [69]. A supercapacitor cell consists of two electrodes separated by an ionic conductor between them as schematically presented in **Figure 7.13**. The separator (ionic conductor) has to be permeable for ions to allow the charge transfer while being highly electrical resistance. The electrodes are thin coatings applied to metallic collector (e.g. aluminium). The electrodes can be the same in the case of symmetric cells, while for asymmetric electrodes are different. All these components play a major role on the performance of the supercapacitor, and the most decisive primary parameters are electrodes and electrolytes. For example, the electrolyte conductivity plays major role on the equivalent series resistance (ESR). On the other hand, there has been lot of interest in the developments of advanced electrode to improve the overall performance of the capacitors. A wide variety of nanosized materials, and/or their hybrids were studied as potential candidates to replace the graphitic commercial electrode for advance capacitors with enhanced electrochemical performance as summarized in **Table 7.4**. The main aim was to reduce the size and increase the contact between the active material and the current collector. Nanomaterials having large surface area can therefore increase contact with current collector to reduce the resistance. In this section we will discuss the application of nanosized materials as either electrode or part of the electrode (**Figure 7.13**).

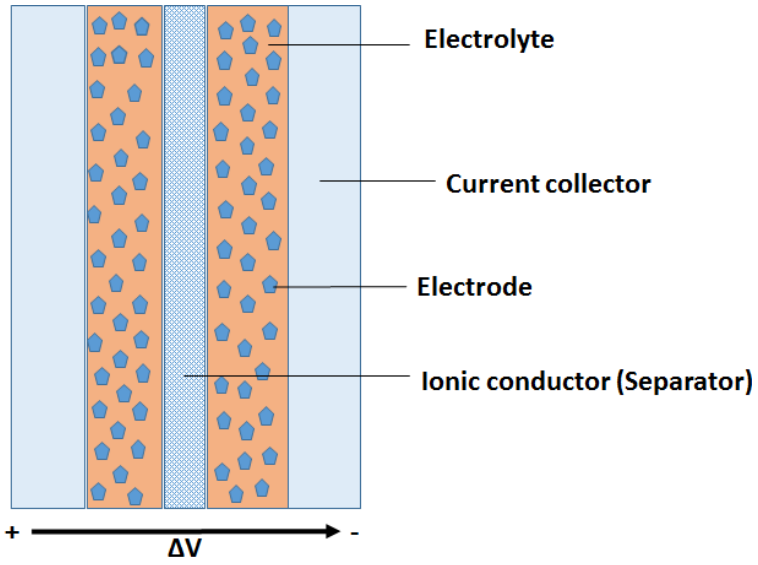

Figure 7.13 Schematic presentation of symmetric supercapacitor

7.3.4.1 Carbon materials as electrode materials

Carbon materials with their special features such as high conductivity, relatively low cost and an industrial production processes which makes them easily accessible were most studied materials as electrode for supercapacitors. Due to their large surface area activated carbon has been widely used as one of the potential electrode [67], however other carbon materials such as graphene nanosheets and carbon nanotubes has been also studied in order to enhance the performance of the capacitors [68].

7.3.4.1.1 Graphene

Graphene has received much interest due to their unique properties, namely large surface area, good flexibility, good electrical conductivity, good thermal and chemical stability for various applications especially for large-scale energy storage. Graphene oxide (GO) produced from natural flake graphite with modified Hummers' method which yield GO sheets with thickness around 1 nm was also studied in [70]. These sheets were used as substrate to grow polyaniline (PANI) nanowires arrays as supercapacitor electrode. Reaching a specific capacitance of 555 F g^{-1} at a discharge current density of 0.2 A g^{-1} confirmed the synergistic effect between PANI

nanowires and GO as potential electrode for supercapacitors. Conductive polymers have a tendency of shrinking and swelling during charging/discharging cycling which affects the performance of the supercapacitors which limit their commercialization [67,70]. It was found that the incorporation of the GO improved the stability of the electrode for more than 2000 cycles with capacitance retention of 92% [70]. Due to the performance brought by graphene and polyaniline (PANI) opens door for their application in flexible electrode with regard to the advancements in technology. These flexible electrodes have a potential as novel energy storage for flexible portable electronic devices, namely roll-up display, electronic paper, stretchable integrated circuits, and wearable systems for personal multimedia, computing, or medical devices. A graphene/polyaniline composite paper prepared by *in situ* anodic electro-polymerization of aniline monomers into polyaniline film on graphene paper to produce a highly flexible, highly conductive and electrochemical activity free-standing composite electrode as shown in **Figure 7.14** was reported in [71]. It was found that the material exhibited the gravimetric capacitance of 233 F g^{-1} (~135 F cm^{-3}) showing their potential as electrode for capacitors. Most recent study based on reduced graphene oxide/polypyrolle/cellulose hybrid papers also justified the possibility of using conductive polymers to induce the flexibility and stability of the supercapacitor electrodes [72]. Introducing natural material, which is cellulose in this case, to serve as supporting frame for RGO-PPy nano-architecture clearly indicate the possibility of introducing third cheaper material to enhance the performance of the electrode, especially mechanical strength to avoid the mechanical failure during service. It was reported that the resulting hybrid was highly flexible and showed high electrochemical activity when tested in a three electrode configuration–(i.e. areal capacitance of 1.20 F cm^{-2} at 2 mA cm^{-2}). Moreover, excellent cycling stability with capacitance retention of ~90% after 5000 times was obtained.

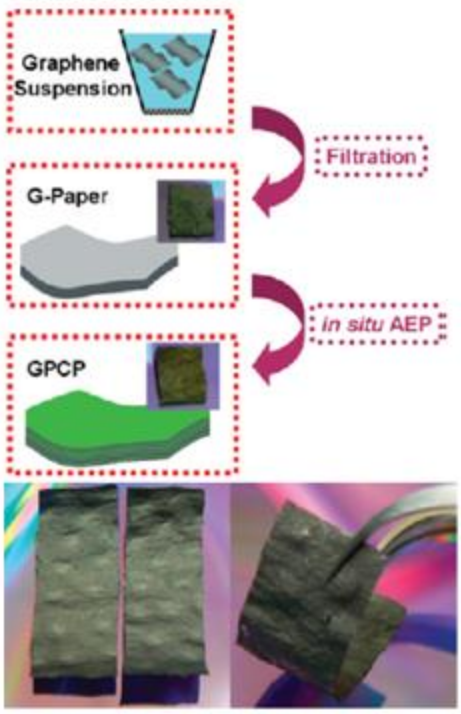

Figure 7.14 (top) Illustrative fabrication process and (bottom) digital camera images of (left) two freestanding G-papers (30 mm × 10 mm) and right a flexible G-paper. Reprinted with permission from [71]. Copyright (2009) American Chemical Society.

Yet doping of graphene with electron donors and acceptors can be applied to enhance its performance as electrode [73-75]. GO obtained by Hummer's method followed by heating in microwave reactor was doped with nitrogen (18 wt%) resulting in a maximum specific capacitance of 461 Fg^{-1} [74]. A facile hydrothermal method with the assistance of amphoteric salt can also be utilized to introduce nitrogen on graphene sheets. However, in this case the specific capacity only reached 242 F g^{-1} at the current density of 1 A g^{-1} with cyclability retention of 97.6% after 5000 cycles [73]. Much higher capacity retention (99.7%) was recently reported by Zhu *et al*. [75] using nitrogen-doped graphene decorated with iron nanorings ($Fe_3)_4$NRs/NH_2-RGO) after 1000 cycles.

One of the major problems that affect the performance of the graphene-based electrodes is restacking of the sheets which reduce the effective surface area. The introduction of the polymers such polypyrrole can intercalate between the sheets and keep them apart which can improve the

electrochemical activity of these graphene-based electrodes. In [76] electrochemical polymerization of pyrrole (PPy) on partially exfoliated graphene sheets on top of graphite foil electrode (Ex-GF) was carried out in the presence of sulfonated aromatic compounds (viz. 1,5-naphthalene disulfonate (NDS) and 2-naphthalene sulfonate (NMS) for 'permanent' doping anions to afford dual doped PPy which anchors partial exfoliated graphene to construct Ex-GF/PPy-NDS and Ex-GF/PPy-NMS electrode. Ex-GF/PPy-NDS and Ex-GF/PPy-NMS displayed specific conductance of 351 and 322 F g^{-1}, respectively. This was ascribed to the open structure of Ex-GF/PPy-NDS and synergistic effects between the components.

Another suitable solution to overcome restacking of the graphene sheets relies on the utilization of metal oxides as spacers [77-79]. Recent study conducted on manganese dioxide nanorods intercalated between graphene oxide (rGO-MnO_2) justified the possibility of using such hybrid materials can enhance the overall electrochemical properties [77]. The nanocomposite hybrid displayed superior specific conductance of 468.48 F g^{-1} when compared to the pure manganese (358.23 Fg^{-1}) at the same current density. This hybrid nanocomposite had a retention capacity of 78.4% as compared to 46.22% for pure MnO_2. Despite that high capacity retention (93.5% after 10000 cycles) were also reported by Zhong *et al*. [79] using 3D graphene oxide/MnO_2 nanocomposites, however they managed to reach a maximum capacity of 278.5 F g^{-1} at current density 1 A g^{-1}. On the other hand, inclusion of silver (Ag) into MnO_2 and GO (Ag/MnO2/rGO) resulted in a specific capacitance of 467.5 F g^{-1} at a scan rate of 5 mV s^{-1} [78]. This hybrid did not show any degeneration after 1000 cycles at the scan rate of 80 mVs^{-1}.

Hybrid composites based on graphene was also studied as an alternative to enhance the electrochemical properties [80-82]. Graphene nanosheets-tungsten composite as an alternative electrode for supercapacitors was reported in [80]. It was reported that the composite material performed better than pure tungsten-based electrode (~32.4 F g^{-1}) by reaching 143.6 F g^{-1} (343%) at a current density of 0.1 A g^{-1}. A chemical deposition of gold nanoparticles into the pores of three-dimensional nitrogen-doped graphene nanosheets was recently reported in [82]. A maximum specific capacitance of 168.6 F g^{-1} at a current density of 1 A g^{-1} with retention of ~97% of the initial capacitance after 500 cycles was achieved. This was attributed to the synergistic effect of gold nanoparticles and hierarchically porous nitrogen-doped graphene. Fan *et al*. [81] also studied the sandwich composite comprise of carbon nanotubes (CNT)/graphene nanosheets. Three-dimensional (3D) CNT/graphene sandwich (CGS) structures with CNT as

pillars grown in between the graphene layers by chemical vapor deposition (CVD) method. GCS was applied as an electrode in supercapacitor and a maximum capacitance of 385 F g^{-1} was obtained at a scan rate of 10 mV s^{-1} in 6 M KOH aqueous solution. This was attributed to the presence of CNT in between the graphene sheets which act as 'spacer' to allow the diffusion of electrolyte ions resulting in improvement of the electrochemical properties. Furthermore, the CNT forms an interconnection with graphene providing conductive network within the sheets reducing the resistance of the electrode.

7.3.4.1.2 Porous carbon materials

Activated carbons have been the most studied carbon material [67,68]. This is as a result of the cost related to the activated and their large specific area. These materials are usually obtained from carbon-rich natural sources by heat treatment in an inert atmosphere (carbonization) and chemical treatment. The chemical process involves oxidation of the carbon-rich material in hot alkali or acidic medium. As a result, the carbon material become more porous with large surface area ranging between 1000-2000 m^2 g^{-1}. One of the limitations of these materials is control over the pore size distribution which hurdles their fully exploitation. It is noteworthy mentioning that most of the commercially available devices include carbon active based electrodes. Very recent study by Peng *et al*. [83] showed that nitrogen-doping of microporous carbon from natural plant (pomelo mesocarps) can enhance the electrochemical properties. Pomelo mesocarps was used to produce porous carbon nanosheets by heat treatment at 800°C under nitrogen flow. It was reported that nitrogen-doping resulted in high specific conductance (~245 F g^{-1} at 0.5 A g^{-1}) and stability in Na_2SO_4 for 10000 cycles and retained 96.5% maximum capacitance. Clearly, natural materials can be applied as a source of carbon to produce low cost supercapacitors electrodes or even in other energy storage applications [83-85]. Mesoporous carbon from lignin was activated by potassium hydroxide (KOH) and carbon dioxide (CO_2) as supercapacitor electrode [84]. It was reported that the CO_2 and KOH activated carbon had large surface area (~1148 m^2 g^{-1} and pore volume of 1.0 cm^3g^{-1}) and displayed the specific capacitance of 102.3 F g^{-1} and 91.7 F g^{-1}, respectively. Rice-husks and beet sugar to produce micro- and mesoporous activated carbon was studied by Kumagai *et al*. [86]. The specific conductance reached ~116 and 106 F g^{-1} at scanning rate of 5 mV s^{-1} for activated carbon from both rice husks and beet as well as rice husk,

respectively. Nitrogen-containing activated carbon was reported in [87] using silk fibroins as the carbon source. Application of adequate heat treatment turned the nitrogen atoms from peptides bonds to the silk carbons in the form of nitrogen-containing functional groups. A maximum specific capacitance of 52 F g^{-1} was achieved.

Electrospinning is one of the techniques that afford to produce fibres with diameters ranging from several micrometers to few nanometers. It was recently recognized that electrospinning can be utilized to produce the mats with nanoporous structure with large surface area as self-standing supercapacitor electrode. This can be achieved by electrospinning suitable polymers followed by carbonization by heating in a furnace [88]. In [88] a self-supported and binder-free microporous polyimide (PI)-based carbon fibers were fabricated by electrospinning from a blend of polyvinyl (PVP) and poly acryl amide (PAA). A maximum specific capacitance of 215 F g^{-1} based on symmetrical two electrode supercapacitor at a current density of 0.2 A g^{-1} was achieved.

7.3.4.1.3 Carbon nanotubes

CNT with the unique properties such as large surface area, excellent electronic, mechanical and chemical properties open doors for a wide variety of applications. These materials are often produced by catalytic decomposition of hydrocarbons. Depending on the fabrication process and the conditions applied two carbon nanotubes can be obtained, namely multi-walled nanotubes (MWCNTs) and single-walled nanotubes (SWCNTs). The freestanding CNT were produced by chemical deposition vapor (CVD) as an electrode for electrochemical double layer capacitors (EDLCs) [89]. Cyclic voltammogram (CV) was almost rectangular-shaped indicating good capacitive behaviour with relatively low equivalent series resistance (ESR). The specific conductance from the galavanosatic charge-discharge curve was 51 F g^{-1}. Similar study based on multi-walled CNT achieved a maximum capacitance of 20 F g^{-1} [90]. Interestingly, the specific power density reached a value of 30 kW kg^{-1}. Moreover, the electrode displayed fairly ideal voltammograms even at high scan rate of 1000 mVs^{-1} which corroborate the applicability of freestanding CNTs as potential electrodes for supercapacitors.

The combination of CNT with metal oxides was also studied to enhance the electrochemical properties [91-93]. A combination of CNT and MnO_2 was studied by Chou *et al*. [91] by electrodepositing the MnO_2 nanowires onto CNT paper using a cyclic voltammetric technique.

The specific capacitance of the CNT/MnO_2 composite (~129 Fg^{-1}) was superior to pure CNT (32 F g^{-1}) at the scan rate of 5 mVs^{-1}. In this case CNT acted as a good conductive layer allowing the MnO_2 fibres to facilitate the movement of the electrolytes active materials. The material displayed a good cyclability with 88% retention of initial capacitance after 3000 cycles. This opens doors for the composite based on CNT and metal oxides in flexible materials as compared to non-flexible powdered based composites materials. A porous flexible capacitor based on CNT/MnO_2 was recently reported by Du *et al.* [94]. The authors used the vacuum filtering method to produce a hybrid of CNT/MnO_2 nanotubes (NT) which exhibited volumetric capacitance of 5.1 F cm^{-3} and a high energy density of 0.45 mWh cm^{-3}. Their results clearly corroborate the application of these flexible materials for high performance power supplies in wearable electronic devices. Yet another method to produce flexible energy storage materials include the use of conductive polymers/CNT composites as compared to the powder-based rigid composites [95].

7.3.4.2 Metal oxides

Metal features unique valuable properties such as high specific capacitance and conductivity making them suitable candidates for electrode fabrication of high density energy supercapacitors. Various metal oxides such as RuO_2, IrO_2, MnO_2, NiO, Co_2O, SnO_2, V_2O_5 or MnO_x have been explored for electrode fabrication [96-101]. Amongst all, ruthenium and manganese oxides are the most studied, thus are the only ones discussed in the following subsections. The mechanisms behind the energy storage in mainly from the fast faradic redox reactions that occur between the oxides and the electrolyte.

7.3.4.2.1 Manganese oxides (MnO_2)

MnO_2 is considered as one of the most promising materials for fabrication of electrodes in capacitors at fairly low cost; and it is environmentally friendly with high theoretical capacitance value (~1110 F g^{-1}). The charge storage of manganese oxides relies on pseudocapacitive reactions on the surface and in the bulk of the electrode. The reaction involves a reversible redox transitions which include the exchange of protons and/or cations with the electrolyte and

transitions between the Mn(III)/Mn(II), Mn(IV)/Mn(III) and Mn(IV)/Mn(IV). This can be expressed as the following **Equation (7.7):** [102, 103]

$$MnO_2 + C^+ + e^- \leftrightarrow MnOOC \qquad \textbf{(7.7)}$$

where C^+ are metal cations/protons from the electrolyte (Li^+, Na^+, K^+). Since the physical and chemical structure of MnO_2 affect pseudocapacitive much work has been done to improve the overall performance. This is as a result of limited specific capacitance of MnO_2 (100-200 F g^{-1}), lack of structural stability and long-term cyclability. It was recognized that the cyclability is mainly defined by the microstructure, while the specific capacitance relies on chemical hydrated state. Much efforts have been dedicated to the synthesis of the MnO_2 with desirable morphology, chemistry and crystal structure. For example, for highly crystalline MnO_2 the ion exchange is limited due to loss of surface area, but there is an increase in conductivity. In turn, there is tradeoff between these two parameters (ion exchange and conductivity) which requires special attention to control the synthesis conditions [103]. The effect of the crystal structure on the specific capacitance is well discussed in the review paper published by Wei *et al*. [104]. This well documented review clearly discussed on how the preparation processes which changes the crystal structure of MnO_2 which in turn affect the specific capacitance of the resulting material. The most suitable solution to overcome the shortcomings of MnO_2 is to include the substrate which is highly conductive and highly porous [104]. Various materials such as graphene oxide [79], carbon nanotube [102] and electrospun carbon nanofibers [105] have been investigated as potential substrate for MnO_2. Moreover, additional nanoparticles were incorporated to enhance the electrochemical performance of MnO_2-based electrodes [78]. For instance, Ma *et al*. [78] decorated MnO_2/graphene oxide with silver nanoparticles to produce a ternary nanocomposite system. In this case, the MnO_2 nanoparticles were grown on graphene oxide followed by co-reduction of Ag^+ and graphene oxide (GO). It was reported that the *in situ* formed Ag and MnO_2 nanoparticles were well-distributed on the surface of reduced GO giving rise a maximum capacitance of 467.5 F g^{-1} at a scan rate of 5 mV s^{-1} which was superior to that of MnO_2/rGO (293.2 F g^{-1}). Moreover, the nanocomposites did not show any degeneration after 1000 cycles at a scan rate of 80 mV s^{-1}. The inclusion of other nanoparticles improves the electrical conductivity which enhances the electron transfer of active materials. It can be concluded that

MnO_2 have a potential of being a part of the next generation of energy storage materials with regard to its performance especially when combined with other conductive materials. For example, very recent study based on MnO_2 nanoflake/CNT core-shell particles as electrode for supercapacitors in [102] justified the enhancement of electrochemical performance of the hybrid nanocomposites. The MnO_2 coating on CNT particles was obtained by the reduction of $KMnO_4$ in the presence of CNT particles. This method involves two stages: (i) fast nucleation forming amorphous particles, and these particles aggregate in a crystal plane and (ii) come together to form a sheet-like structure through Ostwald ripening as shown in **Figure 7.15**. In comparison with pure CNTs, the MnO_2 coated CNT resulted in compact structure with MnO_2 flakes deposited on top of CNT and the contact with neighbouring MnO_2 was achieved by increasing the time for growth (**Figure 7.15**). The electrochemical performance was evaluated in an aqueous Na_2SO_4 at scanning rate of 5, 10, 20, 50 and 100 mV s^{-1}. A rectangular shaped cyclic voltammetry (CV) curves were obtained even at high scanning rate corroborating the good electrochemical capacitor behaviour (**Figure 7.16**). However, at low content of MnO_2 (short growth time) the weak redox was depicted as compared to the higher content (longer growth) in which the peaks were more prominent due to more MnO_2 covering the CNT. A complete coverage of the MnO_2 onto CNT at higher content led to redox reaction on the MnO_2 surface which involves manganese ions Mn^{4+} and Mn^{3+}. This reaction involves the exchange of alkali cations or protons from electrolyte, which is expressed as $MnO_2 + X^+ \leftrightarrow MnOOX$, where X^+ is Na^+ or H^+. The maintenance of the CV curves even at high scanning rate was attributed to a strong bonding between MnO_2 nanoflakes on the CNT surface and low enough interfacial resistance between MnO_2 and CNTs. It was reported that the higher MnO_2 content led to high current density than the lower MnO_2 content as well as CNT particles. The specific conductance from galvanostatic charge-discharge indicated that the higher MnO_2 (370 Fg^{-1}) was superior to lower MnO_2 content (147 Fg^{-1}) as well as bare CNTs (26 Fg^{-1}) at current density of 0.5 Ag^{-1} (**Figure 17**). A comparison between bare MnO_2, low content MnO_2/CNT and high content MnO_2/CNT cyclic performance up to 4000 cycles was performed to evaluate their cyclic stability. It found that the composites maintained ~100% of the initial capacitance, whereas the MnO_2 particle electrode revealed decay and exhibited only 7% of the initial capacitance as shown in **Figure 7.17**. The decay of MnO_2 was ascribed to the detachment of MnO_2 during insertion/desertion and/or the dissolution of MnO_2 into aqueous electrolyte solution,

corroborating the fact that the inclusion of CNT enhanced reversible charging/discharging reaction without debonding. The energy density and a power density were found to be 27 $Whkg^{-1}$ and 225 Wkg^{-1} for the higher content of MnO_2 composites.

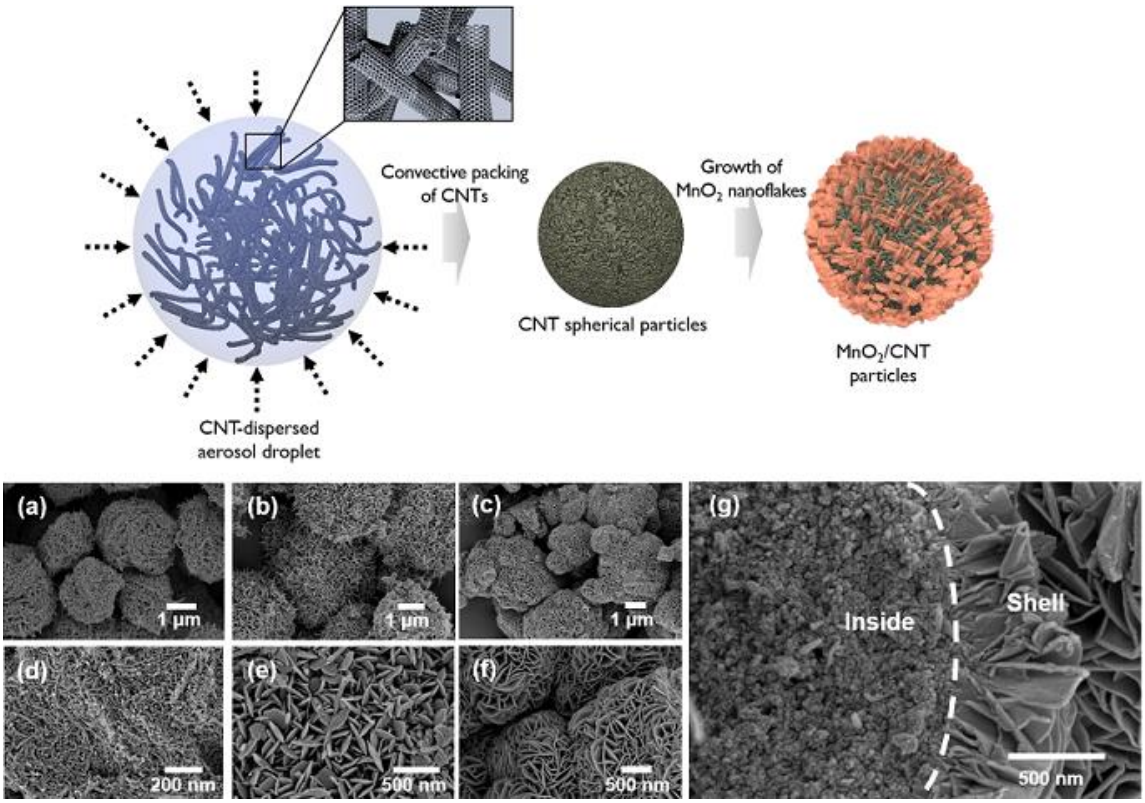

Figure 7.15 **(up) Schematic fabrication of MnO_2/CNT core-shell particles. (down) SEM images of (a) CNT particles, (b) low-MnO_2/CNT core-shell particles, and (c) high-MnO_2/CNT core−shell particles. High-magnitude SEM images of (d) CNT particles, (e) low-MnO_2/CNT core−shell particles, and (f) high-MnO_2/CNT core-shell particles. (g) SEM images of the internal space of the MnO_2/CNT core-shell particle. Reprinted with permission from [102]. Copyright (2009) American Chemical Society.**

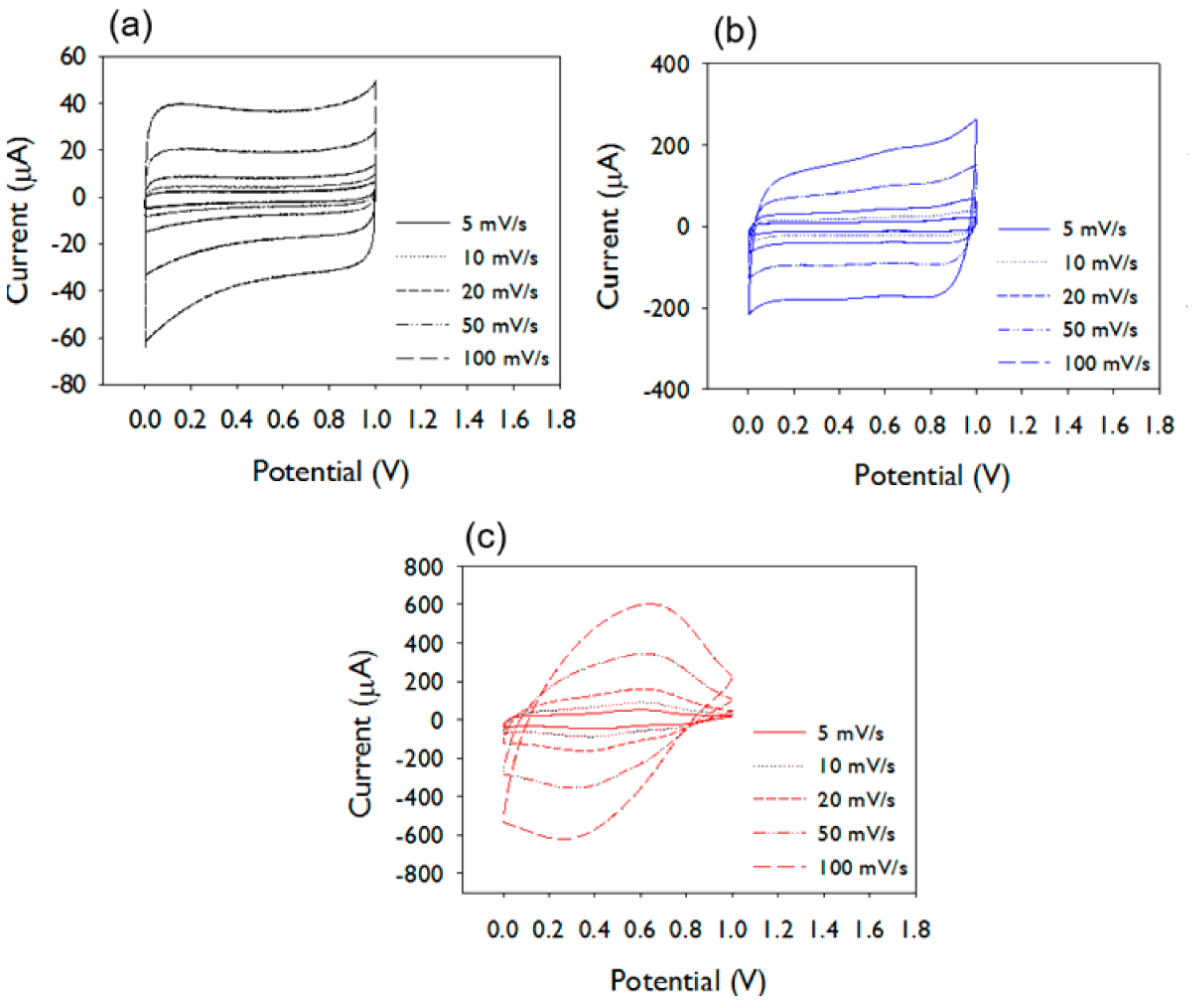

Figure 7.16 **CV curves of (a) the CNT particles, (b) the low-MnO2/CNT core−shell particles, and (c) the high-MnO_2/CNT core−shell particles measured at various scan rates from 5 to 100 mVs^{-1} in a 1 M of Na_2SO_4 electrolyte solution. Reprinted with permission from [102]. Copyright (2009) American Chemical Society.**

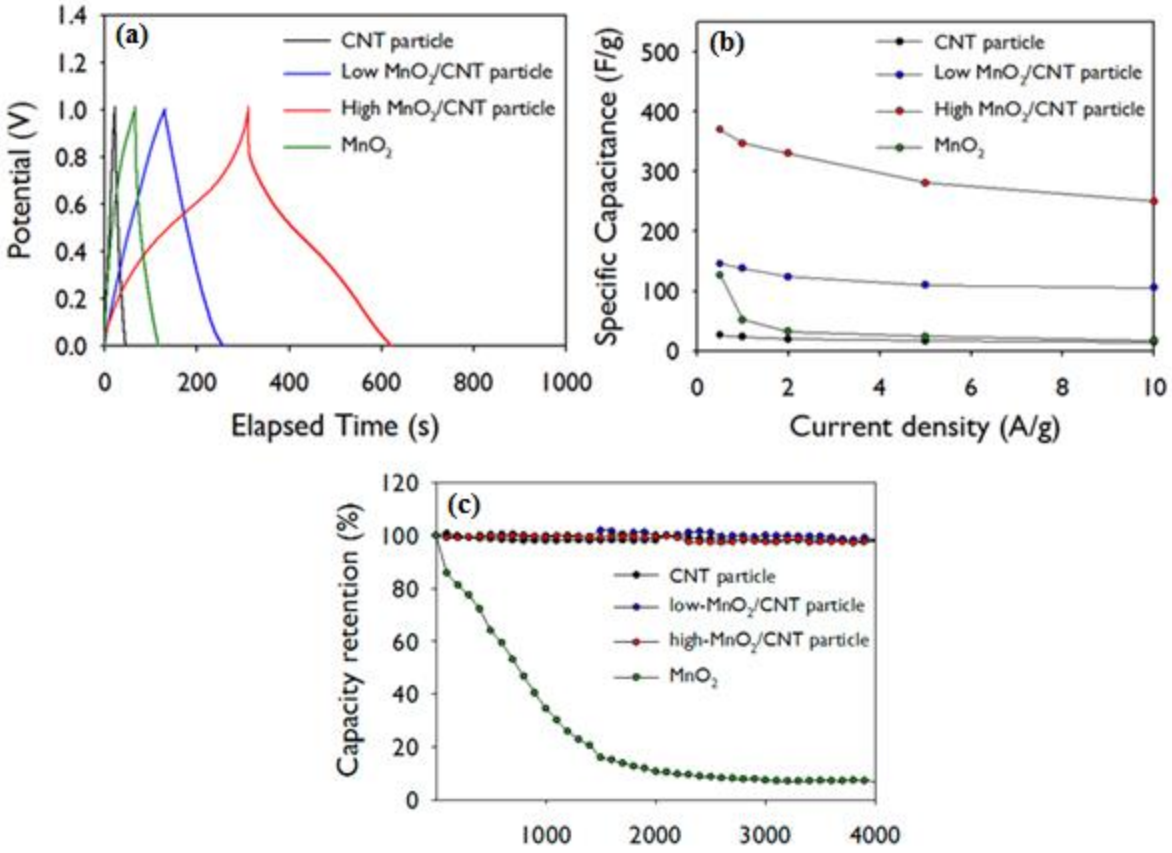

Figure 7.17 **(a) Galvanostatic charge/discharge curves of the CNT particles, low- and high-MnO_2/CNT core−shell particles, and MnO_2 particles at current densities of 1 Ag^{-1}. (b) Calculated specific capacitance of the CNT particles, low- and high-MnO_2/CNT core− shell particles, and MnO_2 particles at various current densities from 0.5 to 10 Ag^{-1}. (c) Cycle performance of the CNT particles, the low- and highMnO_2/CNT core-shell particles and MnO_2 measured at a constant current density of 2 Ag^{-1}. Reprinted with permission from [102]. Copyright (2009) American Chemical Society.**

7.3.4.2.2 Ruthenium oxide

Among other metal oxides, ruthenium oxide is one of the most studied metal oxide. This is as a result of unique properties such as catalytic activities, metallic conductivity, electrochemical reduction-oxidation, field emitting behaviour, high thermal and chemical stability. This pseudocapacitive material has high specific capacitance of about 1000 Fg^{-1} which makes it the

most interesting material [106]. It has a wide potential window and long life cycle. Its pseudo capacitance behaviour of RuO_2 relies on series of oxidation states, namely Ru(IV), Ru(III) and Ru (II). It also features reversible redox processes. The pseudocapacitive process involves the electro-adsorption of protons on the surface of RuO_2 electrode. Generally, it can be expressed as: [69, 106-108].

$$RuO_2 + xH + xe^- \leftrightarrow RuO_{2-x}(OH)_x \qquad \textbf{(7.8)}$$

where $0 \leq x \leq 2$. x changes during insertion/de-insertion occurring at 1.2 voltage window resulting to capacitive behaviour due to ion adsorption following a Frumkin-type isotherm. Brumbach *et al*. [106] studied the nanostructured ruthenium oxide electrode obtained *via* high-temperature molecular templating for use in electrochemical capacitors. They reported unusual behaviour for thermally prepared RuO_2 materials with voltammograms showing that the templated-RuO_2 films (viz. fabricated at high temperatures in the presence of alkyl-thiols) established current 4 times greater than untemplated-RuO_2, which displayed resolvable redox peaks, to broad 'squarish' voltammograms without resolvable peaks, similar to that obtained for hydrous ruthenium oxide and mixed oxides systems. This was attributed to the access granted by the RuO_2 materials for the electrolyte as shown in **Figure 7.18**. The specific capacitance of untemplated RuO_2 was around 200 F g^{-1}, while templated RuO_2 reached values near 400-500 F g^{-1}. These clearly demonstrate that it is possible to reach high capacitance values by using templates which can also be explored for other less expensive metal oxides. The utilized methods afford highly crystalline structure (i.e. leading high conductivity) and densification of the film. SEM images of the templated-films showed a regular array of circular feature, 300 ± 50 nm in diameter, at the surface of the templated-RuO2 (**Figure 7.19A-C**). At lower concentrations of $RuCl_3$ in the precursor solution resulted in a higher density of the circular features as shown in **Figure 7.19A&B** which are more on the subsurface as pores (**Figure 7.19B**). All these features were not observed in the case of untemplated RuO_2; hence they were related to the bubble generated and gas evolved from pyrolysis of the templating material. Moreover, ill-defied pores (~ 4nm in diameter) were observed using TEM (**Figure 7.19D&E**). It was surmised that the chain length of hexane thiol was too short to support formation of a mesophase but influenced the growth of rutile RuO_2 grains and led to a hierarchically porous, nanostructures film which

improved electrolyte access, while protonic and electronic conduction are preserved through the network of hydroxylated RuO_2 nanograins.

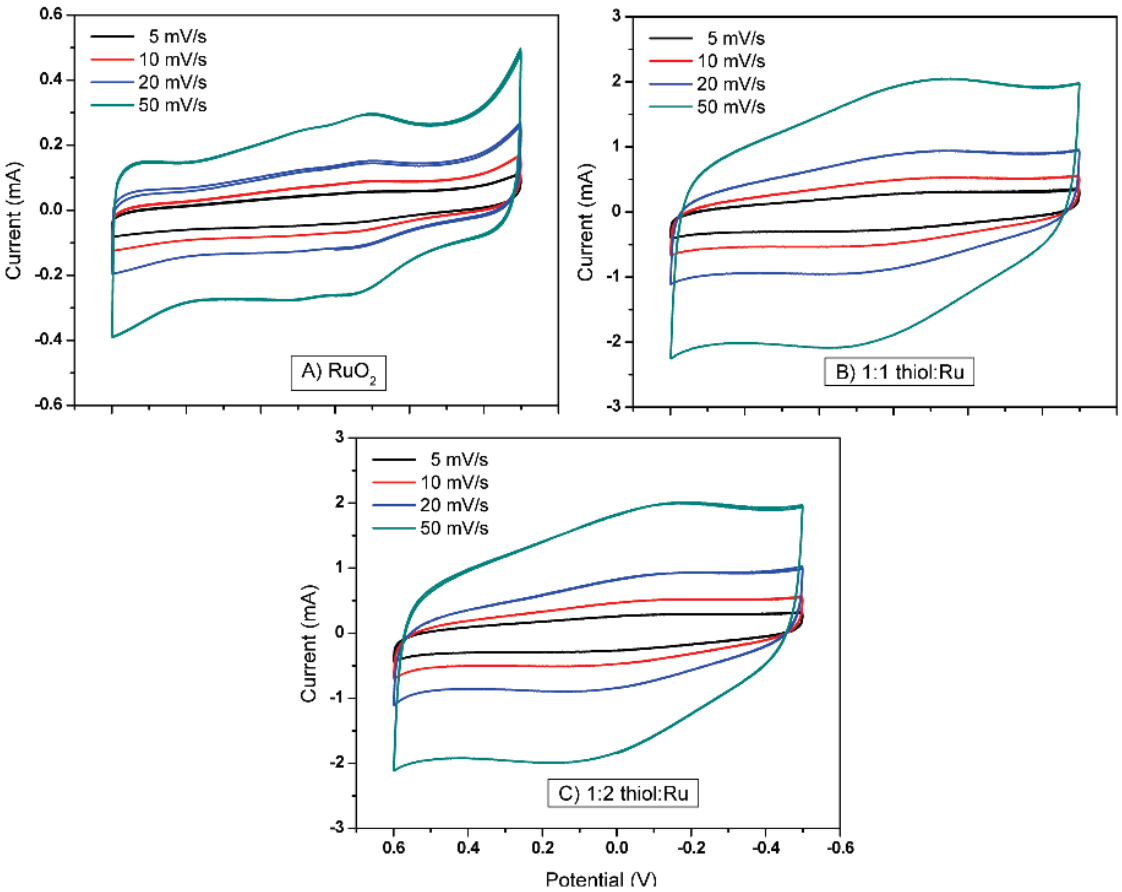

Figure 7.18 **Cyclic voltammetry of ruthenium oxide thin films on titanium are shown for (A) thermally prepared RuO_2, and RuO_2 formed with (B) 1:1 and (C) 1:2 molar additions of thiol relative to Ru in the precursor solution. The electrolyte solution was 1 M H_2SO_4 and potentials are referenced to $Hg/HgSO_4$. Three voltammograms are shown for each scan rate. Scan rates were 5 (black), 10 (red), 20 (blue), and 50 (green) mV/s. Reprinted with permission from [106]. Copyright (2009) American Chemical Society.**

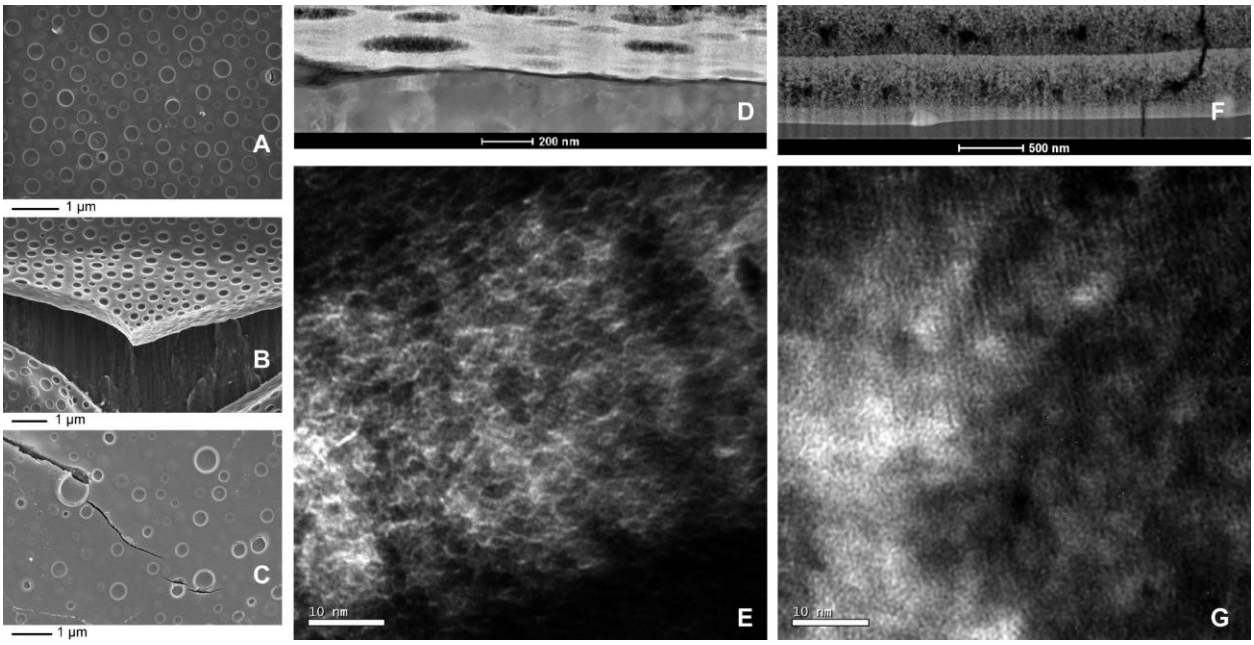

Figure 7.19 **(A-C) Topographical SEM images of templated ruthenium oxide. A regular array of circular features is evident. Subsurface porosity from the gas bubble evolution can be observed in the cross-sectional fragment in B as well as in the TEM cross-section D of the RuO*x* film on titanium. (D) Cross-sectional TEM of the templated ruthenium oxide shows lenticular pores that at (E) higher magnification are composed of an interwoven, fine grained material and nanoscopic porosity. (F, G) TEM cross-sections of untemplated RuO*x* are shown for comparison. Reprinted with permission from [106]. Copyright (2010) American Chemical Society.**

One of the major concerns is the high cost associated with the manufacturing and/or designing an electrode that can exploit the highest capacitance from the least amount of this metal oxide. Therefore, much effort has been dedicated in developing a combine structure of RuO_2 and other electron-conductive electro-chemically stable materials as substrates. Various substrates were studied to come up with best substrate and conducive synthesis process to coat RuO_2 onto a porous substrate especially carbon-based materials since they comprise most of the required properties (e.g. high conductivity and easily prepared into porous large surface area substrate). These include the likes of graphene [109-111]; carbon nanotubes [112,113]; and carbon nanofibers. It was found that it is possible to overcome the shortcomings of RuO_2 especially with regard to the fact that only a part of it participate in the charge-storage mechanism while the

underlying active material remain unreacted. Thus a combination of large surface area materials such as carbon materials with ruthenium oxides can lead to a hybrid nanocomposite with high specific conductance ranging between 150 to 1540 F g^{-1} depending on the thickness of the films. Recent studies showed that the inclusion of the ruthenium into the electrode enhances the electrochemical performance of the overall nanocomposite materials [113,114]. This is attributed to its unique features such as high capacitance (>700 F g^{-1}), low electrochemical resistance (ESR) and long life cycle [113]. One of the principal reasons that hampers the progress of RuO_2 especially towards commercialization is its limited availability and high cost. Despite that the inclusion of these substrates can reduce the overall price of the electrode which facilitates its commercialization in the mere future.

Hydrous ruthenium oxides ($RuO_2.xH_2O$) features high specific capacitance (~900 F g^{-1}) (theoretical 1358 F g^{-1}), and high electrical conductivity (3×10^2 Scm^{-1}) resulting from the inter-particle and interlayer hydrous regions which allows protonic conduction [67,109]. This results in high power and high density supercapacitor. Ternary nanocomposites based on hydrous oxides were also studied aiming to enhance electrochemical properties of the electrode. Using a system comprise of multi-walled carbon nanotubes/RuO_2. xH_2O/ titanium (Ti) as electrode in 1.0 M H_2SO_4 aqueous solution reaches a maximum specific capacitance of 1652 Fg^{-1} at a scan rate of 10 mV s^{-1} [113]. Such behaviour can be related to the nanopore structure of the material which allows fast and reversible faradaic processes on the electrode surfaces. To reduce the price and restacking of the RuO_2 other cheap nanoparticles or sheets can be incorporated between the RuO_2 layers. However, there is some sort of dependency on the ratio between the incorporated particles and RuO_2 in the hybrid material. Thus optimization of the ratio can lead to a high specific conductance [115]. For instance, Deng *et al*. [115] found that 40wt% of RuO_2 was the maximum in the hybrid composite of RuO_2/graphene to achieve a specific conductance of 998 F g^{-1} with excellent cycle stability, and high power density of 20.28 Wh kg^{-1}. Elsewhere, a high specific capacitance of 1017 F g^{-1} was reported using a cheaper vapour grown carbon fibres as a matrix for the dispersion of $RuO_2.xH_2O$ [114]. A core-shell structure of carbon/carbon nanotube supported Ag-Ru nanoparticles can be prepared by using Ag to form a hollow structure which later is replaced by ruthenium. This kind of structures offers more enhancements regarding capacitive behaviour by promoting the proton transportation in RuO_2 due to the shortened diffusion distance [116].

Bendable/flexible capacitors based on RuO_2 were also studied to evaluate their applicability especially for wearable devices [117]. In this case, a binder-free bendable RuO_2 thin film can be

fabricated on top of flexible carbon-based materials such as graphene. Cho *et al*. [117] recently published an article based on RuO_2 fully flexible supercapacitor electrode. The authors prepared a RuO_2 film by coating it onto graphene-coated copper foil using cathodic electroplating technique. It was stated that the electrode exhibited a specific conductance of 1561 F g^{-1} at a scan rate of 5 mV s^{-1} and significantly improved initial capacitance retention of 98% under bent conditions. This electrode exhibited a high energy density of ~13 Wh kg^{-1} at a power density of ~21 kW kg^{-1}. All these improvements were attributed to the improved mechanical adhesion between the RuO_2 and the current collector. There was no structural damage after 500 CV cycles.

Other suitable solution to overcome the high cost ruthenium oxides is to utilize synthesizing route that are cheaper and easily accessible. Furthermore, the route has to be user-friendlier and green. Ismail *et al.* [69] studied the use of *Aspalathus linearis* natural extract as a reducing/oxidizing agent and stabilizing agent for synthesizing RuO_2 nanoparticles. In this case they used $RuCl_3.H_2O$, although is extremely destructive to respiratory system, as precursor and mixed with *Aspalathus linearis* natural plant extract and the synthesis was carried out at room temperature. The RuO_2 nanoparticles were deposited on the nickel foam (NiF), 450 g m^{-2} as 3D template. They observed Faradaic redox peaks around 0.28 and 0.38 V for the NiF/RuO2 as the result of adsorption/desorption of electrolyte K^+ at the surface of RuO_2 which follows **Equation 7.8.** The CV curves confirmed a reversible electron-transfer process demonstrating that the capacitance was associated with charge storage of RuO_2 in KOH aqueous electrolyte due to rapid intercalation of alkali metal cations K^+ in the electrode during reduction and oxidation processes. The calculated specific capacitance for RuO_2/NiF reached 750, 685, 630, 600 and 480 F g^{-1} at the current density of 10, 25, 50, 75, and 100 A g^{-1}, respectively. The cycle efficiency reached 97% retention of initial capacitance over 500 recharge/discharge cycles justify the applicability of this material for long-term. The excellent pseudocapacitive properties and high cycling stability was attributed to the high electrical conductivity of NiF and RuO_2 as well as 3D porous structure of the nickel foam which provided easy access to ions from the electrolyte at the electrode/electrolyte interface.

Table 7.4 Summary of recent results from selected studies of the capacitors based on nanomaterials

Active material	BET surface area ($m^2 g^{-1}$)	Csp ($F g^{-1}$)	Scan rate ($mV s^{-1}$)	C retention (%)	cycles	Refs.
Micro- and mesoporous activated carbon (from Rice Husks and Beet)	1357	116 ± 2	10.5 ± 0.2	-		[86]
Micro- and mesoporous activated carbon (rice husk)	1442	106 ± 6	7.4 ± 0.4	-		[86]
Fe_3O_4 NRs/NH_2-RGO		145	-	99.7	1000	[75]
Porous graphitic biomass carbon (PGMC)	1732	222	-	84	5000	[85]
MnO_2 nanoflakes/CNT		370	-	~100	4000	[102]
RuO_2/graphene		998		94%	1000	[115]
RuO_2/Carbon fibre	13	824	1000	97	300	[114]
Core-shell Ag-Ru nanoparticles/ carbon/CNT		819.9				[116]
RuO_2/activated carbon	1552	180.2				[96]

nanofiber (ACNF)						
Bendable RuO_2/Graphene/Cu		1494	5			[117]
RuO_2/Cu		1891	5			[117]
RuO_2/graphene /CNT foam	743	507	-	106	8100	[109]

7.4 Concluding remarks

The desire for a portable electronic device has pushed the technological enhancements in rechargeable solid-state batteries. It has been explained in these chapter that a battery is composed of various electrochemical cells that are linked to provide the required voltage and capacity. Generally, a cell consists of a positive and negative electrode separated by electrolyte solution containing dissociated salts. One of the most well-known rechargeable batteries is the lithium ion (LIB) and sodium-ion batteries whereby the ions move from the positive electrode to the negative electrode during charging and back during discharging. We have reviewed recent progress in electrochemical applications of lithium ion, supercapacitors and sodium ion batteries. Different nanostructured materials (viz borophene, graphene, carbon nanotubes, porous carbon materials and metal oxides) have been used as electrode material for lithium ion, supercapacitors and sodium ion batteries. Amongst the above mentioned nanostructured materials, graphene have been mostly used in the three systems discussed in this chapter either as an anode or cathode electrode. The advantages of using graphene as one of the electrode are due to its high surface area, ultra-thin thickness, excellent thermal conductivity and good chemical functionality. Furthermore, graphene structure has controllable surface chemical groups which are advantageous for variety of applications in comparison to well-known nanoparticles such carbon nanotubes and graphite. Graphene, as a negative electrode displayed an improved electrochemical performances i.e. reversible capacities up to 540 mAh g^{-1} have been achieved, which is more than the practical value of graphite (350 mAh g^{-1}). The synergistic effect of graphene with other nanoparticles enhances the electrochemical properties further due to (i) graphene nucleating; growing on the surface of other nanoparticles especially metal oxides (ii) other nanoparticles between the layers of the graphene sheet can minimize re-stacking (iii) Graphene can also act as conductive substrate to improve the electrical conductivity as a result the charge transfer of the overall system. Generally, the quality and structure of the nanoparticles depending on the method of preparation used differ from system to system which makes the device behave inconsistently. The above sentence gives a short description generally about the performance of nanostructured materials in energy storage/conversion up to date. For future purposes, attention should be paid to environmental concerns of batteries especially with the addition of nanostructured materials. It is possible that they may come in contact with humans or end up in the environment during their life cycle.

References

1. Pérez-Denicia, E., et al., *Renewable energy sources for electricity generation in Mexico: A review*. Renewable and Sustainable Energy Reviews, 2017. **78**: p. 597-613.
2. Dias, R.A., C.R. Mattos, and J.A. Balestieri, *The limits of human development and the use of energy and natural resources.* Energy Policy, 2006. **34**(9): p. 1026-1031.
3. Sharma, A., et al., *Review on thermal energy storage with phase change materials and applications.* Renewable and Sustainable energy reviews, 2009. **13**(2): p. 318-345.
4. Chieruzzi, M., et al., *Effect of nanoparticles on heat capacity of nanofluids based on molten salts as PCM for thermal energy storage.* Nanoscale research letters, 2013. **8**(1): p. 448.
5. Jones, R., *New materials, old challenges*. 2007, Nature Publishing Group.
6. Strambeanu, N., L. Demetrovici, and D. Dragos, *Natural Sources of Nanoparticles*, in *Nanoparticles' Promises and Risks*. 2015, Springer. p. 9-19.
7. Kim, M., et al., *Synthesis of Nanoparticles by Laser Ablation: A Review*. KONA Powder and Particle Journal, 2017. **34**: p. 80-90.
8. Rohan, J.F., et al., *Energy storage: battery materials and architectures at the nanoscale*, in *ICT-Energy-Concepts Towards Zero-Power Information and Communication Technology*. 2014, Intech.
9. Hannan, M., et al., *A review of lithium-ion battery state of charge estimation and management system in electric vehicle applications: Challenges and recommendations.* Renewable and Sustainable Energy Reviews, 2017. **78**: p. 834-854.
10. Ghimbeu, C.M., et al., *Influence of graphite characteristics on the electrochemical performance in alkylcarbonate LiTFSI electrolyte for Li-ion capacitors and Li-ion batteries.* Journal of The Electrochemical Society, 2013. **160**(10): p. A1907-A1915.
11. Herstedt, M., L. Fransson, and K. Edström, *Rate capability of natural Swedish graphite as anode material in Li-ion batteries.* Journal of power sources, 2003. **124**(1): p. 191-196.
12. Sehrawat, P., C. Julien, and S. Islam, *Carbon nanotubes in Li-ion batteries: A review.* Materials Science and Engineering: B, 2016. **213**: p. 12-40.
13. Li, X. and X. Sun, *Nanostructured Materials for Li-Ion Batteries and Beyond*. 2016, Multidisciplinary Digital Publishing Institute.

14. Sengupta, R., et al., *A review on the mechanical and electrical properties of graphite and modified graphite reinforced polymer composites.* Progress in polymer science, 2011. **36**(5): p. 638-670.
15. Zhang, Y., et al., *Carbon nanomaterials for flexible lithium ion batteries.* Carbon, 2017. **124**: p. 79-88.
16. Wu, Y.-P., E. Rahm, and R. Holze, *Carbon anode materials for lithium ion batteries.* Journal of Power Sources, 2003. **114**(2): p. 228-236.
17. Winter, M., et al., *Insertion electrode materials for rechargeable lithium batteries.* Advanced materials, 1998. **10**(10): p. 725-763.
18. Pumera, M., *Electrochemistry of graphene: new horizons for sensing and energy storage.* The Chemical Record, 2009. **9**(4): p. 211-223.
19. Guo, P., H. Song, and X. Chen, *Electrochemical performance of graphene nanosheets as anode material for lithium-ion batteries.* Electrochemistry Communications, 2009. **11**(6): p. 1320-1324.
20. Wang, G., et al., *Graphene nanosheets for enhanced lithium storage in lithium ion batteries.* Carbon, 2009. **47**(8): p. 2049-2053.
21. Yoo, E., et al., *Large reversible Li storage of graphene nanosheet families for use in rechargeable lithium ion batteries.* Nano letters, 2008. **8**(8): p. 2277-2282.
22. Wang, C., et al., *Electrochemical properties of graphene paper electrodes used in lithium batteries.* Chemistry of Materials, 2009. **21**(13): p. 2604-2606.
23. Lian, P., et al., *Large reversible capacity of high quality graphene sheets as an anode material for lithium-ion batteries.* Electrochimica Acta, 2010. **55**(12): p. 3909-3914.
24. Wan, L., et al., *Graphene nanosheets based on controlled exfoliation process for enhanced lithium storage in lithium-ion battery.* Diamond and Related Materials, 2011. **20**(5): p. 756-761.
25. Caballero, Á. and J. Morales, *Can the performance of graphene nanosheets for lithium storage in Li-ion batteries be predicted?* Nanoscale, 2012. **4**(6): p. 2083-2092.
26. Wu, Z.-S., et al., *Graphene/metal oxide composite electrode materials for energy storage.* Nano Energy, 2012. **1**(1): p. 107-131.
27. Wang, Q., L. Xing, and X. Xue, *SnO2-graphene nanocomposite paper as both the anode and current collector of lithium ion battery with high performance and flexibility.* Materials Letters, 2017. **209**: p. 155-158.

28. Kim, H., et al., *Novel hybrid carbon nanofiber/highly branched graphene nanosheet for anode materials in lithium-ion batteries.* ACS applied materials & interfaces, 2014. **6**(21): p. 18590-18596.
29. Yan, Y., et al., *Facile synthesis of Fe 2 O 3@ graphite nanoparticle composite as the anode for Lithium ion batteries with high cyclic stability.* Electrochimica Acta, 2017.
30. Hassoun, J., et al., *An advanced lithium-ion battery based on a graphene anode and a lithium iron phosphate cathode.* Nano letters, 2014. **14**(8): p. 4901-4906.
31. Mo, R., et al., *Facile Synthesis of Anatase TiO_2 Quantum-Dot/Graphene-Nanosheet Composites with Enhanced Electrochemical Performance for Lithium-Ion Batteries.* Advanced materials, 2014. **26**(13): p. 2084-2088.
32. Peng, C., et al., *Facile ultrasonic synthesis of CoO quantum dot/graphene nanosheet composites with high lithium storage capacity.* ACS nano, 2012. **6**(2): p. 1074-1081.
33. Bai, T., et al., *N-doped carbon-encapsulated MnO@ graphene nanosheet as high-performance anode material for lithium-ion batteries.* Journal of Materials Science, 2017. **52**(19): p. 11608-11619.
34. Chen, Y., et al., *Graphene improving lithium-ion battery performance by construction of NiCo 2 O 4/graphene hybrid nanosheet arrays.* Nano Energy, 2014. **3**: p. 88-94.
35. Tu, F., et al., *Self-Assembly of Bi_2Te_3-Nanoplate/Graphene-Nanosheet Hybrid by One-Pot Route and Its Improved Li-Storage Properties.* Materials, 2012. **5**(7): p. 1275-1284.
36. Yu, Z., et al., *Phosphorus-Graphene Nanosheet Hybrids as Lithium-Ion Anode with Exceptional High-Temperature Cycling Stability.* Advanced Science, 2015. **2**(1-2).
37. Guo, J., et al., *Graphene-encapsulated cobalt sulfides nanocages with excellent anode performances for lithium ion batteries.* Electrochimica Acta, 2015. **167**: p. 32-38.
38. Li, X., et al., *Scalable preparation of mesoporous Silicon@ C/graphite hybrid as stable anodes for lithium-ion batteries.* Journal of Alloys and Compounds, 2017.
39. Wang, Y., et al., *MoS_2-coated vertical graphene nanosheet for high-performance rechargeable lithium-ion batteries and hydrogen production.* NPG Asia Materials, 2016. **8**: p. e268.
40. Kim, H., et al., *Recent Progress in Electrode Materials for Sodium-Ion Batteries.* Advanced Energy Materials, 2016.
41. Ellis, B.L. and L.F. Nazar, *Sodium and sodium-ion energy storage batteries.* Current Opinion in Solid State and Materials Science, 2012. **16**(4): p. 168-177.

42. Mortazavi, B., et al., *Borophene as an anode material for Ca, Mg, Na or Li ion storage: A first-principle study.* Journal of Power Sources, 2016. **329**: p. 456-461.
43. Shi, L., et al., *Ab initio prediction of borophene as an extraordinary anode material exhibiting ultrafast directional sodium diffusion for sodium-based batteries.* Science Bulletin, 2016. **61**(14): p. 1138-1144.
44. Liu, Y., et al., *SnO_2 coated carbon cloth with surface modification as Na-ion battery anode.* Nano Energy, 2015. **16**: p. 399-407.
45. Wang, H., et al., *Nanocrystal growth on graphene with various degrees of oxidation.* Journal of the American Chemical Society, 2010. **132**(10): p. 3270-3271.
46. Yang, X., et al., *Assembly of SnSe Nanoparticles Confined in Graphene for Enhanced Sodium-Ion Storage Performance.* Chemistry-A European Journal, 2016. **22**(4): p. 1445-1451.
47. Zhang, C., et al., *Amorphous phosphorus/nitrogen-doped graphene paper for ultrastable sodium-ion batteries.* Nano letters, 2016. **16**(3): p. 2054-2060.
48. Xiong, X., et al., *Enhancing sodium ion battery performance by strongly binding nanostructured Sb2S3 on sulfur-doped graphene sheets.* ACS nano, 2016. **10**(12): p. 10953-10959.
49. Zhang, F., et al., *SnSe2 2D Anodes for Advanced Sodium Ion Batteries.* Advanced Energy Materials, 2016. **6**(22).
50. Lan, Z., et al., *Investigations on molybdenum dinitride as a promising anode material for Na-ion batteries from first-principle calculations.* Journal of Alloys and Compounds, 2017. **701**: p. 875-881.
51. Mortazavi, M., et al., *Ab initio characterization of layered MoS_2 as anode for sodium-ion batteries.* Journal of Power Sources, 2014. **268**: p. 279-286.
52. Wu, H., et al., *A theoretical study on the electronic property of a new two-dimensional material molybdenum dinitride.* Physics Letters A, 2016. **380**(5): p. 768-772.
53. Liang, P., et al., *Is borophene a suitable anode material for sodium ion battery?* Journal of Alloys and Compounds, 2017. **704**: p. 152-159.
54. Sun, Q., Y. Yang, and Z.-W. Fu, *Electrochemical properties of room temperature sodium–air batteries with non-aqueous electrolyte.* Electrochemistry Communications, 2012. **16**(1): p. 22-25.

55. Zhang, Y., et al., *Identifying a Stable Counter/Reference Electrode for the Study of Aprotic Na-O_2 Batteries.* Journal of The Electrochemical Society, 2016. **163**(7): p. A1270-A1274.
56. Yadegari, H., Q. Sun, and X. Sun, *Sodium-Oxygen Batteries: A Comparative Review from Chemical and Electrochemical Fundamentals to Future Perspective.* Advanced Materials, 2016. **28**(33): p. 7065-7093.
57. Liu, C., et al., *The Growth of NaO2 in Highly Efficient Na-O_2 Batteries Revealed by Synchrotron In Operando X-ray Diffraction.* ACS Energy Letters, 2017.
58. Kwak, W.-J., et al., *Nanoconfinement of low-conductivity products in rechargeable sodium-air batteries.* Nano Energy, 2015. **12**: p. 123-130.
59. Landa-Medrano, I., et al., *Sodium-oxygen battery: steps toward reality.* The journal of physical chemistry letters, 2016. **7**(7): p. 1161-1166.
60. Pinedo, R., et al., *Insights into the chemical nature and formation mechanisms of discharge products in Na-O_2 batteries by means of operando x-ray diffraction.* The Journal of Physical Chemistry C, 2016. **120**(16): p. 8472-8481.
61. Zhang, S., et al., *Graphene nanosheets loaded with Pt nanoparticles with enhanced electrochemical performance for sodium–oxygen batteries.* Journal of Materials Chemistry A, 2015. **3**(6): p. 2568-2571.
62. Yadegari, H., et al., *Three-dimensional nanostructured air electrode for sodium–oxygen batteries: a mechanism study toward the cyclability of the cell.* Chemistry of Materials, 2015. **27**(8): p. 3040-3047.
63. Liu, W., et al., *An enhanced electrochemical performance of a sodium–air battery with graphene nanosheets as air electrode catalysts.* Chemical Communications, 2013. **49**(19): p. 1951-1953.
64. Jian, Z., et al., *High capacity Na-O_2 batteries with carbon nanotube paper as binder-free air cathode.* Journal of Power Sources, 2014. **251**: p. 466-469.
65. Elia, G.A., I. Hasa, and J. Hassoun, *Characterization of a reversible, low-polarization sodium-oxygen battery.* Electrochimica Acta, 2016. **191**: p. 516-520.
66. Sun, Q., et al., *Self-stacked nitrogen-doped carbon nanotubes as long-life air electrode for sodium-air batteries: Elucidating the evolution of discharge product morphology.* Nano Energy, 2015. **12**: p. 698-708.
67. González, A., et al., *Review on supercapacitors: technologies and materials.* Renewable and Sustainable Energy Reviews, 2016. **58**: p. 1189-1206.

68. Simon, P. and A. Burke, *Nanostructured carbons: double-layer capacitance and more.* The electrochemical society interface, 2008. **17**(1): p. 38.
69. Ismail, E., et al., *Green biosynthesis of ruthenium oxide nanoparticles on nickel foam as electrode material for supercapacitor applications.* RSC Advances, 2016. **6**(90): p. 86843-86850.
70. Xu, J., et al., *Hierarchical nanocomposites of polyaniline nanowire arrays on graphene oxide sheets with synergistic effect for energy storage.* ACS nano, 2010. **4**(9): p. 5019-5026.
71. Wang, D.-W., et al., *Fabrication of graphene/polyaniline composite paper via in situ anodic electropolymerization for high-performance flexible electrode.* ACS nano, 2009. **3**(7): p. 1745-1752.
72. Wan, C., Y. Jiao, and J. Li, *Flexible, highly conductive, and free-standing reduced graphene oxide/polypyrrole/cellulose hybrid papers for supercapacitor electrodes.* Journal of Materials Chemistry A, 2017. **5**(8): p. 3819-3831.
73. Wang, D., et al., *A general approach for fabrication of nitrogen-doped graphene sheets and its application in supercapacitors.* Journal of colloid and interface science, 2014. **417**: p. 270-277.
74. Gopalakrishnan, K., A. Govindaraj, and C. Rao, *Extraordinary supercapacitor performance of heavily nitrogenated graphene oxide obtained by microwave synthesis.* Journal of Materials Chemistry A, 2013. **1**(26): p. 7563-7565.
75. Zhu, F., et al., *Synthesis of Fe_3O_4 Nanorings/Amine-Functionalized Reduced Graphene Oxide Composites as Supercapacitor Electrode Materials in Neutral Electrolyte.* Int. J. Electrochem. Sci, 2017. **12**: p. 7197-7204.
76. Song, Y., J.-L. Xu, and X.-X. Liu, *Electrochemical anchoring of dual doping polypyrrole on graphene sheets partially exfoliated from graphite foil for high-performance supercapacitor electrode.* Journal of power sources, 2014. **249**: p. 48-58.
77. Parveen, N., et al., *Manganese dioxide nanorods intercalated reduced graphene oxide nanocomposite toward high performance electrochemical supercapacitive electrode materials.* Journal of Colloid and Interface Science, 2017. **506**: p. 613-619.
78. Ma, L., et al., *Ag nanoparticles decorated MnO_2/reduced graphene oxide as advanced electrode materials for supercapacitors.* Chemical Engineering Journal, 2014. **252**: p. 95-103.

79. Zhong, J., et al., *Preparation of 3D Reduced Graphene Oxide/MnO_2 Nanocomposites through a Vacuum-Impregnation Method and Their Electrochemical Capacitive Behavior.* ChemElectroChem, 2017. **4**(5): p. 1088-1094.
80. Cai, Y., et al., *Graphene nanosheets-tungsten oxides composite for supercapacitor electrode.* Ceramics International, 2014. **40**(3): p. 4109-4116.
81. Fan, Z., et al., *A three-dimensional carbon nanotube/graphene sandwich and its application as electrode in supercapacitors.* Advanced materials, 2010. **22**(33): p. 3723-3728.
82. Jiang, L., et al., *Promoting the Electrochemical Performances by Chemical Depositing of Gold Nanoparticles inside Pores of 3D Nitrogen-doped Carbon Nanocages.* ACS Applied Materials & Interfaces, 2017.
83. Peng, H., et al., *Nitrogen-doped interconnected carbon nanosheets from pomelo mesocarps for high performance supercapacitors.* Electrochimica Acta, 2016. **190**: p. 862-871.
84. Saha, D., et al., *Studies on supercapacitor electrode material from activated lignin-derived mesoporous carbon.* Langmuir, 2014. **30**(3): p. 900-910.
85. Gong, Y., et al., *Highly porous graphitic biomass carbon as advanced electrode materials for supercapacitors.* Green Chemistry, 2017. **19**(17): p. 4132-4140.
86. Kumagai, S., M. Sato, and D. Tashima, *Electrical double-layer capacitance of micro- and mesoporous activated carbon prepared from rice husk and beet sugar.* Electrochimica Acta, 2013. **114**: p. 617-626.
87. Kim, Y.J., et al., *Easy preparation of nitrogen-enriched carbon materials from peptides of silk fibroins and their use to produce a high volumetric energy density in supercapacitors.* Carbon, 2007. **45**(10): p. 2116-2125.
88. Le, T., et al., *Preparation of microporous carbon nanofibers from polyimide by using polyvinyl pyrrolidone as template and their capacitive performance.* Journal of Power Sources, 2015. **278**: p. 683-692.
89. Ci, L., et al., *Ultrathick freestanding aligned carbon nanotube films.* Advanced Materials, 2007. **19**(20): p. 3300-3303.
90. Du, C., J. Yeh, and N. Pan, *High power density supercapacitors using locally aligned carbon nanotube electrodes.* Nanotechnology, 2005. **16**(4): p. 350.
91. Chou, S.-L., et al., *Electrodeposition of MnO_2 nanowires on carbon nanotube paper as free-standing, flexible electrode for supercapacitors.* Electrochemistry Communications, 2008. **10**(11): p. 1724-1727.

92. Pan, H., J. Li, and Y. Feng, *Carbon nanotubes for supercapacitor.* Nanoscale research letters, 2010. **5**(3): p. 654.
93. Xie, X. and L. Gao, *Characterization of a manganese dioxide/carbon nanotube composite fabricated using an in situ coating method.* Carbon, 2007. **45**(12): p. 2365-2373.
94. Du, L., et al., *Flexible supercapacitors based on carbon nanotube/MnO_2 nanotube hybrid porous films for wearable electronic devices.* Journal of Materials Chemistry A, 2014. **2**(41): p. 17561-17567.
95. Meng, C., C. Liu, and S. Fan, *Flexible carbon nanotube/polyaniline paper-like films and their enhanced electrochemical properties.* Electrochemistry communications, 2009. **11**(1): p. 186-189.
96. Yang, K.S. and B.-H. Kim, *Highly conductive, porous RuO_2/activated carbon nanofiber composites containing graphene for electrochemical capacitor electrodes.* Electrochimica Acta, 2015. **186**: p. 337-344.
97. Ren, X.-B., et al., *Preparation and characterization of the $Ti/IrO_2/WO_3$ as supercapacitor electrode materials.* Russian Journal of Electrochemistry, 2010. **46**(1): p. 77-80.
98. Lee, J.Y., et al., *Nickel oxide/carbon nanotubes nanocomposite for electrochemical capacitance.* Synthetic metals, 2005. **150**(2): p. 153-157.
99. Zhang, J., et al., *Ultrafine SnO_2 nanocrystals anchored graphene composites as anode material for lithium-ion batteries.* Materials Research Bulletin, 2015. **68**: p. 120-125.
100. Deng, L., et al., *Graphene/VO_2 hybrid material for high performance electrochemical capacitor.* Electrochimica Acta, 2013. **112**: p. 448-457.
101. Tang, K., et al., *Self-reduced VO/VO_x/carbon nanofiber composite as binder-free electrode for supercapacitors.* Electrochimica Acta, 2016. **209**: p. 709-718.
102. Gueon, D. and J.H. Moon, *MnO_2 nanoflake-shelled carbon nanotube particles for high-performance supercapacitors.* ACS Sustainable Chemistry & Engineering, 2017. **5**(3): p. 2445-2453.
103. Wei, J., N. Nagarajan, and I. Zhitomirsky, *Manganese oxide films for electrochemical supercapacitors.* Journal of materials processing technology, 2007. **186**(1): p. 356-361.
104. Wei, W., et al., *Manganese oxide-based materials as electrochemical supercapacitor electrodes.* Chemical society reviews, 2011. **40**(3): p. 1697-1721.

105. Kim, B.-H., *MnO_2 decorated on electrospun carbon nanofiber/graphene composites as supercapacitor electrode materials.* Synthetic Metals, 2016. **219**: p. 115-123.
106. Brumbach, M.T., et al., *Nanostructured ruthenium oxide electrodes via high-temperature molecular templating for use in electrochemical capacitors.* ACS applied materials & interfaces, 2010. **2**(3): p. 778-787.
107. Ramani, M., et al., *Synthesis and characterization of hydrous ruthenium oxide-carbon supercapacitors.* Journal of The Electrochemical Society, 2001. **148**(4): p. A374-A380.
108. Borenstein, A., et al., *Carbon-based composite materials for supercapacitor electrodes: a review.* Journal of Materials Chemistry A, 2017.
109. Wang, W., et al., *Hydrous ruthenium oxide nanoparticles anchored to graphene and carbon nanotube hybrid foam for supercapacitors.* Scientific reports, 2014. **4**.
110. Leng, X., et al., *Electrochemical capacitive behavior of RuO_2/graphene composites prepared under various precipitation conditions.* Journal of Alloys and Compounds, 2015. **653**: p. 577-584.
111. Lin, N., et al., *Hydrothermal synthesis of hydrous ruthenium oxide/graphene sheets for high-performance supercapacitors.* Electrochimica Acta, 2013. **99**: p. 219-224.
112. Kim, Y.-T., K. Tadai, and T. Mitani, *Highly dispersed ruthenium oxide nanoparticles on carboxylated carbon nanotubes for supercapacitor electrode materials.* Journal of Materials Chemistry, 2005. **15**(46): p. 4914-4921.
113. Hsieh, T.-F., et al., *Hydrous ruthenium dioxide/multi-walled carbon-nanotube/titanium electrodes for supercapacitors.* Carbon, 2012. **50**(5): p. 1740-1747.
114. Lee, B.J., et al., *Carbon nanofibre/hydrous RuO_2 nanocomposite electrodes for supercapacitors.* Journal of Power Sources, 2007. **168**(2): p. 546-552.
115. Deng, L., et al., *RuO_2/graphene hybrid material for high performance electrochemical capacitor.* Journal of Power Sources, 2014. **248**: p. 407-415.
116. Wang, P., et al., *Carbon/carbon nanotube-supported RuO_2 nanoparticles with a hollow interior as excellent electrode materials for supercapacitors.* Nano Energy, 2015. **15**: p. 116-124.
117. Cho, S., et al., *Bendable RuO_2/graphene thin film for fully flexible supercapacitor electrodes with superior stability.* Journal of Alloys and Compounds, 2017. **725**: p. 108-114.